DNA 5289F

METHODS OF FORCE IDENTIFICATION FOR EARTH PENETRATORS

T. Belytschko
18 Longmeadow Road
Winnetka, Illinois 60093

1 January 1980

Final Report for Period 1 July 1976—1 December 1977

CONTRACT No. DNA 001-76-C-0167

APPROVED FOR PUBLIC RELEASE;
DISTRIBUTION UNLIMITED.

THIS WORK SPONSORED BY THE DEFENSE NUCLEAR AGENCY
UNDER RDT&E RMSS CODE B344076464 Y99QAXSB04815 H2590D.

Prepared for
Director
DEFENSE NUCLEAR AGENCY
Washington, D. C. 20305

Destroy this report when it is no longer needed. Do not return to sender.

PLEASE NOTIFY THE DEFENSE NUCLEAR AGENCY, ATTN: STTI, WASHINGTON, D.C. 20305, IF YOUR ADDRESS IS INCORRECT, IF YOU WISH TO BE DELETED FROM THE DISTRIBUTION LIST, OR IF THE ADDRESSEE IS NO LONGER EMPLOYED BY YOUR ORGANIZATION.

UNCLASSIFIED

SECURITY CLASSIFICATION OF THIS PAGE (When Data Entered)

REPORT DOCUMENTATION PAGE

READ INSTRUCTIONS BEFORE COMPLETING FORM

1. REPORT NUMBER: DNA 5289F	2. GOVT ACCESSION NO.: AD-A095 122
3. RECIPIENT'S CATALOG NUMBER:	
4. TITLE (and Subtitle): METHODS OF FORCE IDENTIFICATION FOR EARTH PENETRATORS	5. TYPE OF REPORT & PERIOD COVERED: Final Report. ~~for Period~~ 1 Jul 76—1 Dec 77
	6. PERFORMING ORG. REPORT NUMBER:
7. AUTHOR(s): T. N. Belytschko	8. CONTRACT OR GRANT NUMBER(s): DNA 001-76-C-0167
9. PERFORMING ORGANIZATION NAME AND ADDRESS: T. Belytschko, 18 Longmeadow Road, Winnetka, Illinois 60093	10. PROGRAM ELEMENT, PROJECT, TASK AREA & WORK UNIT NUMBERS: Subtask Y99QAXSB048-15
11. CONTROLLING OFFICE NAME AND ADDRESS: Director, Defense Nuclear Agency, Washington, D.C. 20305	12. REPORT DATE: 1 January 1980
	13. NUMBER OF PAGES: 56
14. MONITORING AGENCY NAME & ADDRESS (if different from Controlling Office): B048	15. SECURITY CLASS (of this report): UNCLASSIFIED
	15a. DECLASSIFICATION/DOWNGRADING SCHEDULE:

16. DISTRIBUTION STATEMENT (of this Report)

Approved for public release; distribution unlimited.

17. DISTRIBUTION STATEMENT (of the abstract entered in Block 20, if different from Report)

18. SUPPLEMENTARY NOTES

This work sponsored by the Defense Nuclear Agency under RDT&E RMSS Code B344076464 Y99QAXSB04815 H2590D.

19. KEY WORDS (Continue on reverse side if necessary and identify by block number)

Penetrators
Dynamics
Inverse Problem
Identification Problem

20. ABSTRACT (Continue on reverse side if necessary and identify by block number)

A procedure is developed for identifying the forces on the nose of a penetrator vehicle from strain time histories at selected points in the vehicle in off-normal impact of the vehicle. The vehicle nose is idealized as a rigid body, the remainder as a deformable rod. The following forces are considered: axial forces, transverse forces in two planes, and bending moments. The deformation response of the vehicle is assumed to be linear. The identification is separated into the identification of the flexural forces and axial forces.

DD FORM 1 JAN 73 1473 EDITION OF 1 NOV 65 IS OBSOLETE

UNCLASSIFIED

SECURITY CLASSIFICATION OF THIS PAGE (When Data Entered)

392 212

20. ABSTRACT (Continued)

Any coupling arising from body forces due to rigid body motion must be neglected. The methods were tested by using analytic and finite element methods to generate strain records and comparing the identified and applied load. Finally, the method was used to identify the loads on a reverse ballistics experiment; the identified loads were evaluated by applying them to a finite element model of the penetrator and comparing the response of this model to the experimental results.

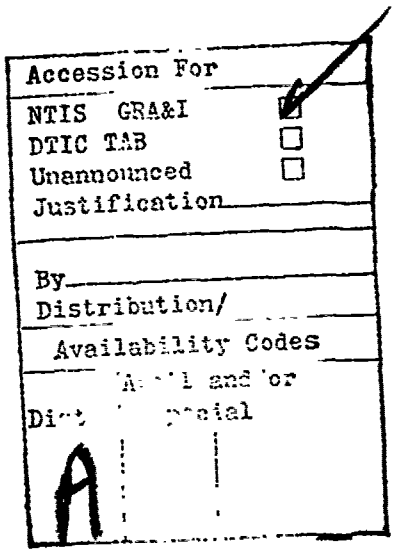

TABLE OF CONTENTS

LIST OF ILLUSTRATIONS

LIST OF ILLUSTRATIONS (cont.)

SECTION I

INTRODUCTION

This report is concerned with the following inverse problem: given the strain response of a penetrator vehicle as functions of time, identify the loads as functions of time. The objective of this effort is to use experimental records of strains in vehicles to determine the forces sustained by a vehicle during penetration. In this effort, attention is limited to the development of appropriate techniques for the problem and the testing of certain aspects of these techniques by comparison with solutions and experimental results.

The identification problem for off-normal impact is quite complex, for it involves separate flexural and axial effects that arise from loads distributed over a fairly large area. In the present investigation, attention is restricted to the linear response of the vehicle, that is, the strains are assumed to remain small and the response is assumed to be elastic. The vehicle is modeled as a uniform rod with the nose represented by a rigid body. Contact stresses are represented as point loads and moments at the center of mass of this rigid body.

The identification problem is subdivided into two parts: the determination of the axial force and the determination of the flexural forces. A simple procedure is developed so that if the axial strain is known as a function of time at any point along the neutral axis of the vehicle, the axial force on the nose can be determined. The determination of the flexural forces requires that strains be measured at a minimum of two stations along the length of the vehicle; at each station, strains must be measured at three points. The procedures are outlined in Sections 2 through 4. In Section 5 some sample results are given which illustrate the effectiveness of the methods for the axial and flexural problem. The methods are then used to identify the forces for a reverse

ballistics experiment (ref. 1). The results are evaluated by applying these identified loads on a detailed finite element model and comparing computed strains and accelerations to experimental records.

SECTION II

THE FORCE IDENTIFICATION PROBLEM

In its most general terms, the identification problem consists of determining the distribution of normal and tangential loads on the vehicle as a function of time. This identification must be accomplished from strain gauge records at selected points in the vehicle and perhaps one or two accelerometer records. The elements of this problem are illustrated in Fig. 1.

When considered in this degree of generality, the identification problem is horrendously difficult. The reason for this is explained in the following. Consider the pressures at points A and B, shown in Fig. 1, which are called p_n^A and p_n^B, respectively. The response of a strain gauge at C due to the pressures p_n^A and p_n^B will differ because the signal from B will arrive sooner than that from A. However, subsequent to the arrival of the wave from B, there is no way to distinguish whether the signal arrived from A or B, unless a strain gauge is located between A and B.

It is possible to distinguish the signals if the expected depth of penetration is known as function of time. However, if the load is to be determined after partial penetration of the nose, this information is of little help since subsequent to penetration beyond B, both points A and B can be sources. This, in conjunction with practical limitations on the number of available strain gauge records, renders the general problem of distributed load identification impractical.

For purposes of formulating a practical force identification problem, we will limit the endeavor to net resultant forces on a specified segment of the vehicle. The following assumptions are made:

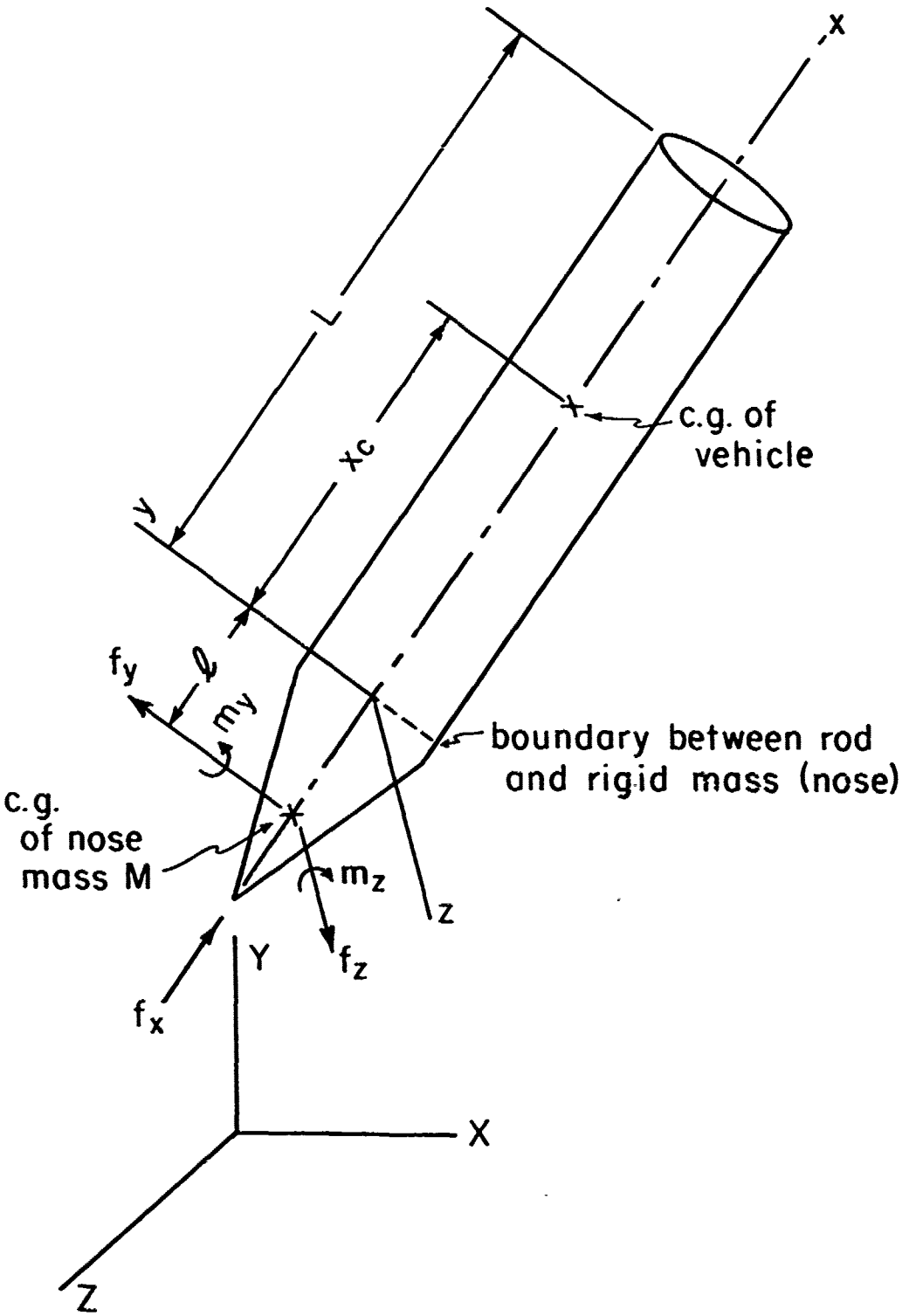

Figure 1. Depiction of general force identification problem for a penetrator.

i. Contact between the vehicle and medium occurs primarily in the nose region; behind the nose, the medium tends to separate from the vehicle.

ii. No significant torques about the vehicles axis are exerted, nor does the vehicle spin about its axis.

The first assumption is based largely on normal impact calculations performed by CRT (ref. 2). In off-normal impact, the DNA-SANDIA (ref. 1) experiments have shown significant backslap, so this assumption limits the method to identification of early loads. Without this assumption the identification problem would become very complex. The second assumption is based on the observation that in impact, no mechanism exists which would exert a torque on the vehicle.

The vehicle is modelled as a uniform elastic bar and the nose represented by a rigid body of finite dimensions. This simplification was used in predicting the response to normal impact of the DNA-SANDIA vehicle (ref. 3) and was quite successful. The model is shown in Fig. 1.

The loads to be identified then consist of the following forces and moments on the nose (rigid-body in the model):

i. the axial force, $f_x(t)$, and transverse forces $f_y(t)$ and $f_z(t)$

ii. the moments $m_y(t)$ and $m_z(t)$.

In order to describe the equations governing this model, it is convenient to introduce two coordinate systems:

i. a moving coordinate system (x,y,z) embedded in the projectile such that x always lies along the axis of the vehicle as shown in Fig. 2, with the origin located at the interface between the rigid body and the deformable bar;

ii. a coordinate system (X,Y,Z) fixed to the target, which is considered inertial.

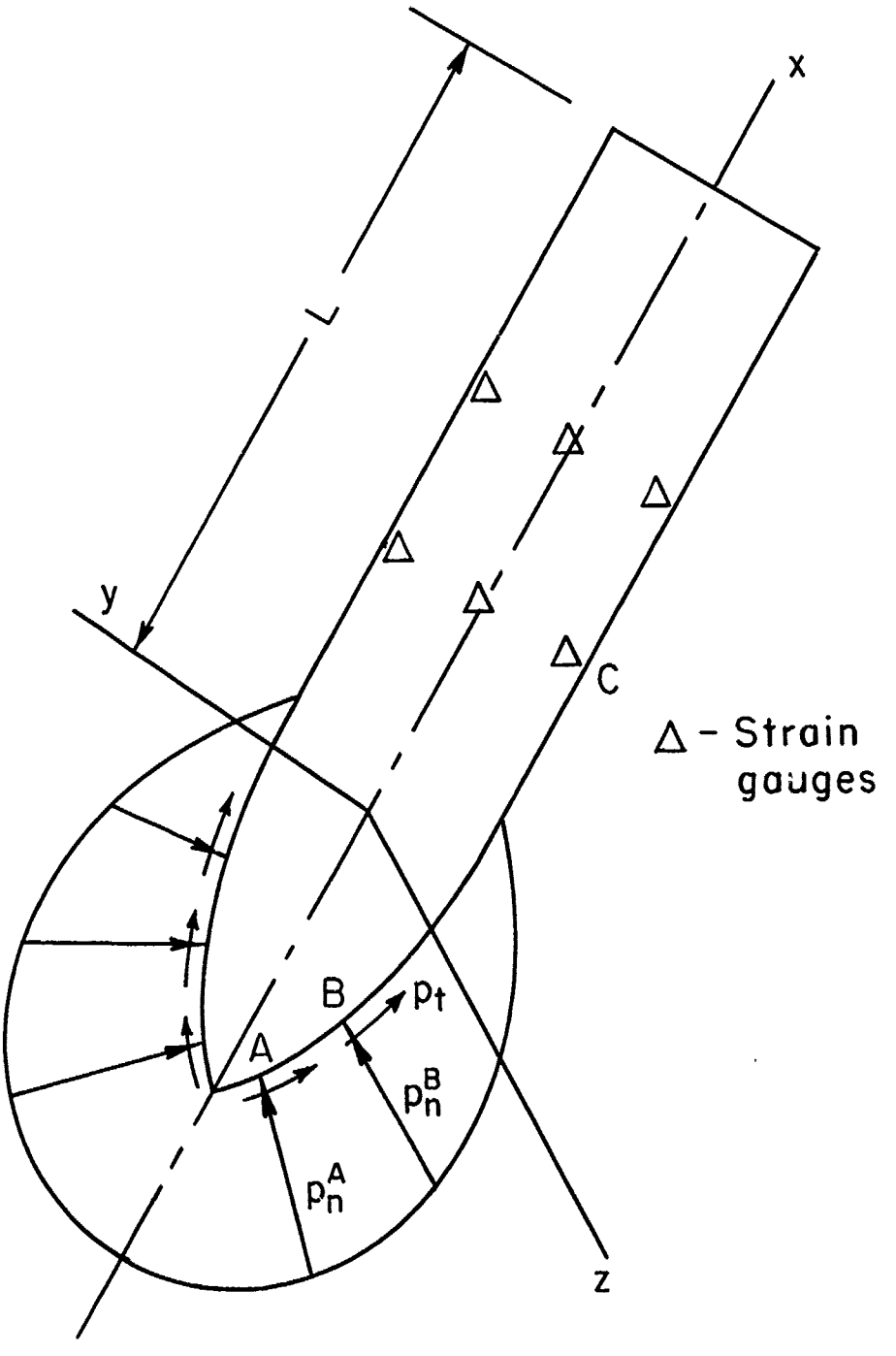

Figure 2. Coordinate systems and nomenclature.

The displacement of a point in the vehicle, $\vec{r}$, relative to the vehicle's coordinates is given by a vector $\vec{v}$ with components v_x, v_y, v_z, which are assumed to be small. The displacement of the center of mass of the vehicle is denoted by $\vec{V}$. The angular velocity and angular acceleration of the vehicle are $\vec{\omega}$ and $\vec{\alpha}$. The acceleration of any point of the vehicle is then

$$\ddot{\vec{R}} = \ddot{\vec{u}} + 2\vec{\omega} \times \dot{\vec{v}} + \vec{\alpha} \times \vec{r} + \vec{\omega} \times (\vec{\omega} \times \vec{r})$$

$$\vec{u} = \vec{V} + \vec{v} \tag{2.1}$$

Since we assume the vehicle is not spinning, its only nonzero angular velocities are ω_y and ω_z. Moreover, the vehicle is considered slender and the rotatory inertia of the cross-section will be neglected. From these assumptions it follows that

$$\vec{r} = \bar{x}\vec{i} \qquad \bar{x} = x - x_c$$

$$\vec{\omega} = \omega_y\vec{j} + \omega_z\vec{k} \tag{2.2}$$

The acceleration components in the (x,y,z) systems are given by

$$\ddot{R}_x = \ddot{u}_x + 2(\omega_y\dot{v}_z - \omega_z\dot{v}_y) - (\omega_y^2 + \omega_z^2)\bar{x} \tag{2.3}$$

$$\ddot{R}_y = \ddot{u}_y + 2\omega_z\dot{v}_x + \alpha_z\bar{x} \tag{2.4}$$

$$\ddot{R}_z = \ddot{u}_z - 2\omega_y\dot{v}_x - \alpha_y\bar{x} \tag{2.5}$$

Linear strength of materials theory will be employed for describing the dynamic deformation response. Simple first order rod theory which neglects the effects of transverse inertia will be used for the axial response. Euler beam theory will be used for the bending response. The cross-section of the vehicle is assumed to be axisymmetric so that the moment of inertia of the cross-section is isotropic. Therefore bending in the x-y planes and in the y-z planes is uncoupled for any choice of the orientation of the y and z coordinates. Moreover, the axial deformation is uncoupled from bending because of the assumption of small displacements.

The governing equations are then

$$c^2 v_{x,xx} = \ddot{R}_x \tag{2.6}$$

$$c_b^2 v_{y,xxxx} = \ddot{R}_y \tag{2.7}$$

$$c_b^2 v_{z,xxxx} = \ddot{R}_z \tag{2.8}$$

where commas denote derivatives. The accelerations are given by Eqs. (2.3) to (2.5) and

ρ = density of vehicle material

E = Young's modulus of vehicle material

A = cross-sectional area

I = moment of inertia of cross section about both the y and z axes

$c^2 = E/\rho$, elastic rod wavespeed

$c_b^2 = EI/\rho A$

By using Eqs. (2.3) to (2.5), Eqs. (2.6) to (2.8) can be written as

$$c^2 v_{x,xx} - \ddot{u}_x = b_x \tag{2.9}$$

$$c_b^2 v_{y,xxxx} - \ddot{u}_y = b_y \tag{2.10}$$

$$c_b^2 v_{z,xxxx} - \ddot{u}_z = b_z \tag{2.11}$$

where

$$b_x = 2(\omega_y \dot{v}_z - \omega_z \dot{v}_y) - (\omega_y^2 + \omega_z^2)\, \bar{x} \tag{2.12}$$

$$b_y = 2\omega_z \dot{v}_x + \alpha_z \bar{x} \tag{2.13}$$

$$b_z = -2\omega_y \dot{v}_x - \alpha_z \bar{x} \tag{2.14}$$

The terms b_x, b_y, and b_z couple Eqs. (2.9) to (2.11). In order to uncouple the equations we assume that these terms vanish. Since the rigid body motion $\vec{v}$ is independent of x,y and z, its derivatives vanish and we can replace Eqs. (2.9) to (2.11) by

$$c^2 u_{x,xx} - \ddot{u}_x = 0 \tag{2.15}$$

$$c_b^2 u_{y,xxxx} - \ddot{u}_y = 0 \tag{2.16}$$

$$c_b^2 u_{z,xxxx} - \ddot{u}_z = 0 \tag{2.17}$$

The displacements u_y and u_z and their second derivatives must be small, but u_x may be arbitrarily large, although its first derivative must also be small. The boundary conditions are

$$A\,E\,u_{x,x} = M\ddot{u} - f_x(t) \qquad \text{at } x = 0$$

$$A\,u_{x,x} = 0 \qquad \text{at } x = L \tag{2.18}$$

$$-E\,I\,u_{y,xxx} = M\,(\ddot{u}_y - \ell\ddot{u}_{y,x}) - f_y(t)$$

$$E\,I\,(u_{y,xx} - \ell u_{y,xxx}) = J\,\ddot{u}_{y,x} - m_z(t) \tag{2.19}$$

$$\text{at } x = 0$$

$$-E\,I\,u_{z,xxx} = M(\ddot{u}_z - \ell\ddot{u}_{z,x}) - f_z(t)$$

$$E\,I\,(u_{z,xx} - \ell u_{z,xxx}) = J\,\ddot{u}_{z,x} + m_y(t) \tag{2.20}$$

$$u_{z,xx} = u_{z,xxx} = 0 \qquad \text{at } x = L$$

where J is the moment of inertia of the rigid body. Initial conditions provide the initial velocity of the projectile.

The strain at any point x,y,z in the structure is given by

$$\varepsilon(x, y, z, t) = u_{x,x} - y\,u_{y,xx} - z\,u_{z,xx} \tag{2.21}$$

The identification problem then consists of the following: given strain histories at selected points x_i, y_i, z_i, determine the forces $f_x(t)$, $f_y(t)$, and $f_z(t)$ and the moments $m_y(t)$ and $m_z(t)$. For convenience, we denote by $\{F(t)\}$ the complete matrix of forces to be determined: $\{f_x, f_y, f_z, m_y, m_z\}$.

When strain records at three different points y_j, z_j are given at any cross section x_i, then Eq. (2.21) can be solved uniquely to yield the response $\{r(t)\} = \{u_{x,x}(x_i,t), u_{y,xx}(x_i,t), u_{z,xx}(x_i,t)\}$ provided that the matrix

$$[A] = \begin{bmatrix} 1 & -y_1 & -z_1 \\ 1 & -y_2 & -z_2 \\ 1 & -y_3 & -z_3 \end{bmatrix} \tag{2.23}$$

is not singular

The matrix [A] is singular if and only if all three points are collinear. Thus any triangular arrangement of the points y_j, z_j is sufficient to permit the determination of $\{r(t)\}$.

Once $\{r(t)\}$ is given. The complete identification problem can be subdivided into three uncoupled parts:

i. given $\varepsilon = u_{x,x}(x_i, t)$, determine f_x through Eq. (2.15) and boundary conditions (2.18)

ii. given $u_{y,xx}(x_i, t)$, determine m_z and f_y through Eq. (2.16) and boundary conditions (2.19)

iii. given $u_{z,xx}(x_i, t)$, determine m_y and f_z through Eq. (2.17) and boundary conditions (2.20).

Problem (i) is an axial problem, problems (ii) and (iii) identical flexural problems; they are discussed in Sections 3 and 4, respectively. For two dimensional problems, where the motion of the vehicle is planar, only problems (i) and (ii) need be solved.

SECTION III

AXIAL FORCE IDENTIFICATION

We consider here the problem of the identification of the axial load. The axial response problem is governed by the equations and boundary conditions (subscripts x are omitted in this section)

$$u_{,xx} = \frac{1}{c^2}\ddot{u} \tag{3.1}$$

$$AE\, u_{,x} = M\ddot{u} - f(t) \qquad \text{at } x = 0 \tag{3.2}$$

$$u_{,x} = 0 \qquad \text{at } x = L \tag{3.3}$$

which correspond to Eqs. (2.9) and (2.18). The initial conditions are taken to be

$$u(x,0) = 0 \tag{3.4}$$

$$\dot{u}(x,0) = 0 \tag{3.5}$$

The problem is to obtain the time history of the net force on the nose, f(t), given the axial strain time history at one point.

We will use Laplace transform techniques. Let the Laplace transform of a given variable be denoted by a corresponding upper case letter, i.e. U(x,s) is the Laplace transform u(x,t), so that

$$U(x,s) = \int_0^\infty u(x,t)e^{-st}\,dt \tag{3.6}$$

Similarly E(s) is the Laplace transform of $\varepsilon(t)$, F(s) the Laplace transform of f(t).

Taking the Laplace transform of Eq. (3.1) and noting that the initial conditions are zero, g:

$$U_{,xx}(x,s) = \frac{s^2}{c^2} U(x,s) \tag{3.7}$$

which has the solution

$$U(x,s) = K_1 e^{-sx/c} + K_2 e^{sx/c} \tag{3.8}$$

The Laplace transforms of the boundary conditions, (3.2) and (3.3), give

$$AEU_{,x}(0,s) = M s^2 U(0,s) - F(s) \tag{3.9}$$

$$U_{,x}(L,s) = 0 \tag{3.10}$$

Substituting Eq. (3.8) into Eqs. (3.9) and (3.10) yields two linear, algebraic equations in K_1 and K_2, the solution of which is

$$K_1 = e^{2Ls/c} F(s)/G(s) \tag{3.11}$$

$$K_2 = F(s)/G(s) \tag{3.12}$$

where

$$G(s) = s \left[\left(Ms + \frac{AE}{c}\right) e^{2Ls/c} + \left(Ms - \frac{AE}{c}\right) \right] \tag{3.13}$$

From Eq. (3.8), it also follows that the Laplace transform of the strain at any point x_i is given by

$$\mathcal{E}(x_i,s) = \frac{s}{c}\,[-K_1 e^{-sx_i/c} + K_2 e^{sx_i/c}] \tag{3.14}$$

Substituting Eqs. (3.11) and (3.12) into (3.14) and solving for F(s) yields

$$F(s) = \frac{1}{sH(s)}\; c\,\mathcal{E}(x_i,s)\; G(s) \tag{3.15a}$$

$$H(s) = e^{x_i s/c} - e^{(2I-x_i)s/c} \tag{3.15b}$$

Substituting Eq. (3.13) into Eq. (3.15), we can write the latter as

$$F(s) = \frac{\mathcal{E}(x_i,s)}{H(s)}\,[(Mcs + AE)e^{2Ls/c} + (Mcs - AE)] \tag{3.16}$$

The time domain counterpart of Eq. (3.16) is

$$f(t + \frac{x_i}{c}) - f(t + \frac{2L-x_i}{c}) = Mc\dot{\varepsilon}(x_i,t) - AE\varepsilon(x_i,t)$$

$$+ Mc\dot{\varepsilon}(x_i,t + \frac{2L}{c}) + AE\varepsilon(x_i,t + \frac{2L}{c}) \tag{3.17}$$

Thus by shifting in time by $(2L-x_i)/c$, we obtain from Eq. (3.17) that

$$f(t) = f(t - 2\,(L - x_i)/c) + AE\,[\varepsilon(x_i,t - \frac{2L-x_i}{c}) - \varepsilon(x_i,t + \frac{x_i}{c})]$$

$$- Mc\,[\dot{\varepsilon}(x_i,t + \frac{x_i}{c}) - \dot{\varepsilon}(x_i,t - \frac{2L-x_i}{c})] \tag{3.18}$$

From the above equation, it is apparent that once an axial strain record is known at any given point, the force history can be determined. Although a Laplace transform approach has been used, from the time shifts that occur in the equations, it is apparent that this result follows from the nature of the solution to the wave equation. The solution always consists of a wave induced by the force which moves to the left and an image moving to the right, shifted in time by L/c, which maintains the stress free condition on the right end of the rod. The Laplace transform approach serves to formalize these results.

SECTION IV

FLEXURAL FORCE IDENTIFICATION

From each flexural equation, two quantities, a force and a moment, must be determined. The flexural equation and associated boundary conditions, Eqs. (2.10) or (2.11), and (2.19) or (2.20), can be written

$$w_{,xxxx} + \frac{1}{c_b^2} \ddot{w} = 0 \tag{4.1}$$

$$w_{,xxx} = c_1 (\ddot{w} - \ell \ddot{w}_{,x}) - f \qquad \text{at } x = 0 \tag{4.2}$$

$$w_{,xx} - \ell w_{,xxx} = c_2 \ddot{w}_{,x} - m \qquad \text{at } x = 0 \tag{4.3}$$

$$w_{,xx} = 0 \qquad \text{at } x = L \tag{4.4}$$

$$w_{,xxx} = 0 \qquad \text{at } x = L \tag{4.5}$$

where

$$c_b^2 = \frac{EI}{\rho A} \tag{4.6}$$

$$c_1 = \frac{M}{EI} \tag{4.7}$$

$$c_2 = \frac{J}{EI} \tag{4.8}$$

The problem is to identify f(t) and m(t) from records of the curvature $w_{,xx}(x_i,t)$. As in Section 3, we will use a Laplace transform approach and denote the Laplace transform by upper case letters.

Taking the Laplace transform of Eq. (4.1) yields

$$W_{,xxxx} + \frac{s^2}{c_b^2} W = 0 \tag{4.9}$$

for which the solution is

$$W(x,s) = K_1 e^{\gamma_1 x} + K_2 e^{-\gamma_1 x} + K_3 e^{\gamma_2 x} + K_4 e^{-\gamma_2 x} \tag{4.10}$$

$$\gamma_1 = (1 + j)\sqrt{\frac{s}{2c_b}} \qquad \gamma_2 = (1 - j)\sqrt{\frac{s}{2c_b}} \tag{4.11}$$

and K_i are functions of s, and

$$j = \sqrt{-1} \tag{4.12}$$

The boundary conditions at $x = 0$ and $x = L$ can be written in partitioned matrix form in terms of $W(x,s)$ as follows

$$\begin{bmatrix} & \\ [H_{11}] & [H_{12}] \\ & \\ [H_{21}] & [H_{22}] \\ & \end{bmatrix} \begin{Bmatrix} K_1 \\ K_2 \\ K_3 \\ K_4 \end{Bmatrix} = \begin{Bmatrix} F \\ M \\ 0 \\ 0 \end{Bmatrix} \tag{4.13}$$

$$[H_{11}] = \begin{bmatrix} c_1 s^2 (1 - \gamma_1 \ell) + \gamma_1^3 & c_1 s^2 (1 + \gamma_1 \ell) - \gamma_1^3 \\ \gamma_1^2 (1 - \gamma_1 \ell) - c_2 s^2 \gamma_1 & \gamma_1^2 (1 + \gamma_1 \ell) + c_2 s^2 \gamma_1 \end{bmatrix} \tag{4.14a}$$

$$[H_{12}] = \begin{bmatrix} c_1 s^2 (1 - \gamma_2 \ell) + \gamma_2^3 & c_1 s^2 (1 + \gamma_2 \ell) - \gamma_2^3 \\ \gamma_2^2 (1 - \gamma_2 \ell) - c_2 s^2 \gamma_2 & \gamma_2^3 (1 + \gamma_2 \ell) + c_2 s^2 \gamma_2 \end{bmatrix} \tag{4.14b}$$

$$[H_{21}] = \gamma_1^2 \begin{bmatrix} e^{\gamma_1 \ell} & e^{-\gamma_1 \ell} \\ \gamma_1 e^{\gamma_1 \ell} & -\gamma_1 e^{-\gamma_1 \ell} \end{bmatrix} \tag{4.14c}$$

$$[H_{22}] = \gamma_2^2 \begin{bmatrix} e^{\gamma_2 \ell} & e^{-\gamma_2 \ell} \\ \gamma_2 e^{\gamma_2 \ell} & -\gamma_2 e^{-\gamma_2 \ell} \end{bmatrix} \tag{4.14d}$$

The transform of the response, at any point x_i, is given by

$$W_{,xx}(x_i,s) = K_1 \gamma_1^2 e^{\gamma_1 x_i} + K_2 \gamma_1^2 e^{-\gamma_1 x_i} + K_3 \gamma_2^2 e^{\gamma_2 x_i} + K_4 \gamma_3^2 e^{-\gamma_2 x_i} \tag{4.15}$$

If the curvature is given at two points, x_1 and x_2, then we can write

$$\begin{Bmatrix} W(x_1,s) \\ W(x_2,s) \end{Bmatrix} = \begin{bmatrix} [L_{11}] & [L_{12}] \end{bmatrix} \begin{Bmatrix} K_1 \\ K_2 \\ K_3 \\ K_4 \end{Bmatrix} \tag{4.16}$$

From Eq. (4.13), it follows that

$$\begin{Bmatrix} K_3 \\ K_4 \end{Bmatrix} = -[H_{22}]^{-1} [H_{21}] \begin{Bmatrix} K_1 \\ K_2 \end{Bmatrix} \tag{4.17}$$

Hence

$$\begin{Bmatrix} W(x_1,s) \\ W(x_2,s) \end{Bmatrix} = \left([L_{11}] - [L_{12}] [H_{22}]^{-1} [H_{21}] \right) \begin{Bmatrix} K_1 \\ K_2 \end{Bmatrix} \tag{4.18}$$

If we call the above square matrix [G], Eqs. (4.14) and (4.18) yield

$$\begin{Bmatrix} F(s) \\ M(s) \end{Bmatrix} = \left([H_{11}] - [H_{12}] [H_{22}]^{-1} [H_{21}] \right) [G]^{-1} \begin{Bmatrix} W(x_1,s) \\ W(x_2,s) \end{Bmatrix} \tag{4.19}$$

An explicit transformation of the above into the time domain is impossible. Instead, the operations of Eq. (4.19) were carried out in the frequency domain, using Fast Fourier Transform algorithms.

The procedure consists of the following. Transforms are obtained of the response $w_{,xx}$ at two points. The transfer function relating the input to the response is then evaluated; its product with the response yields the transform of the forcing function. The inverse transform of the forcing functions are then taken to obtain the forcing functions in the time domain.

The submatrix $[H_{22}]$ is singular at $s = 0$ (rigid body mode) and at the natural frequencies. To make the inversion possible, artificial damping is added to the system. This displaces the zeroes from the imaginary axis and so avoids the singularities.

Note that the number of distinct forces that can be identified depends on the number of response records. Two response records are needed to identify the force and moment on the nose. If backslap is to be identified, it could be represented by an inhomogeneous term in the boundary condition Eq. (4.5); responses at three points along the axis of the vehicle would then be needed.

SECTION V

ILLUSTRATIVE RESULTS

The force identification procedures for the axial force and the flexural forces have been tested through the use of analytic and finite element solutions. Analytic solutions were used to test the procedure as follows: the strain was predicted for a prescribed forcing function at the nose, and this strain was then used as input to the identification procedure. The identified load was then compared with the actual force. The finite element test was similar except that finite element solutions were used rather than an analytical solution to obtain the strains from the forces.

In both tests, the vehicle described in Fig. 3 was used. The first test involved only an axial load with the time history shown in Fig. 4. The responses at x = 7in. and 15in. are shown in Figs. 5 and 6. Figure 7 shows the force as computed from the identification procedure given in Section 3, and compares the results to the applied load. As can be seen, the identified axial load corresponds closely with the actual load. There are some discrepancies at the points at which the slope of the actual load is discontinuous; the identified load at those points tends to smooth over these discontinuities.

The same procedure was repeated with the finite element solution. The finite element solution shows the effect of the vehicle idealization and the sensitivity of the identification procedure to spurious oscillations. Finite element solutions have spectral amplification and cut-offs similar to strain gauges. The identified force is compared to the actual force in Fig. 8. As can be seen, for the finite element solution, the identified force does not correspond as closely to the actual input force as in the case of the analytic

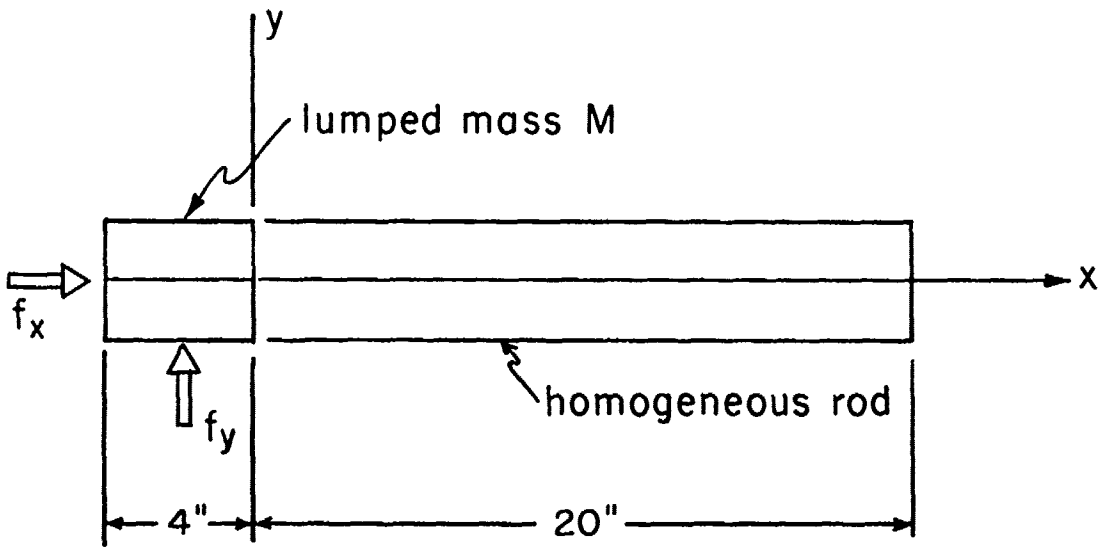

Mg = 12.0 lbs.

A = 4.41 in^2

E = 2.85×10^7 psi

ρ = 0.000732 lb. - sec^2/in^4

Figure 3. Configuration of sample problem.

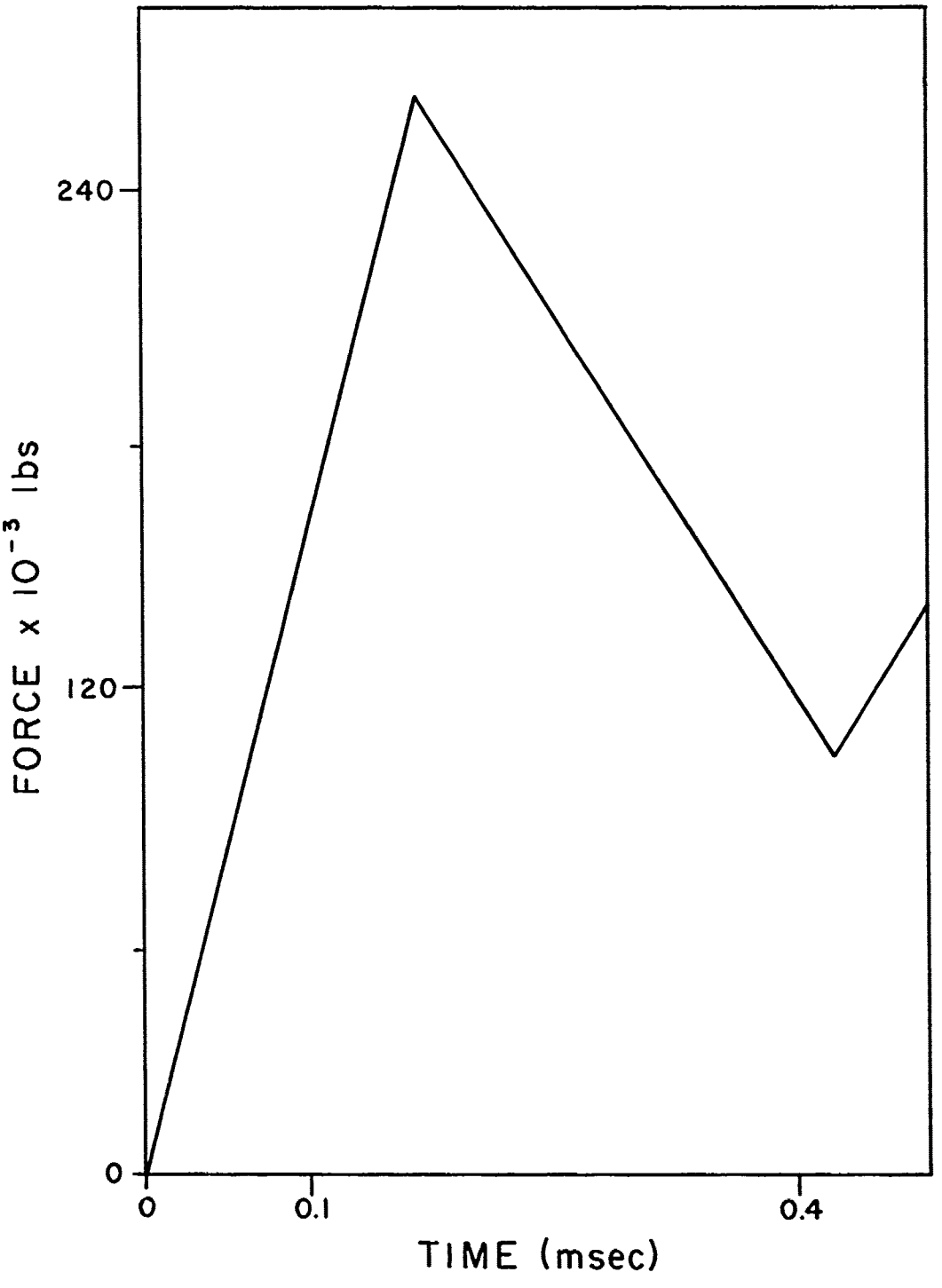

Figure 4. Applied axial force, f(t)

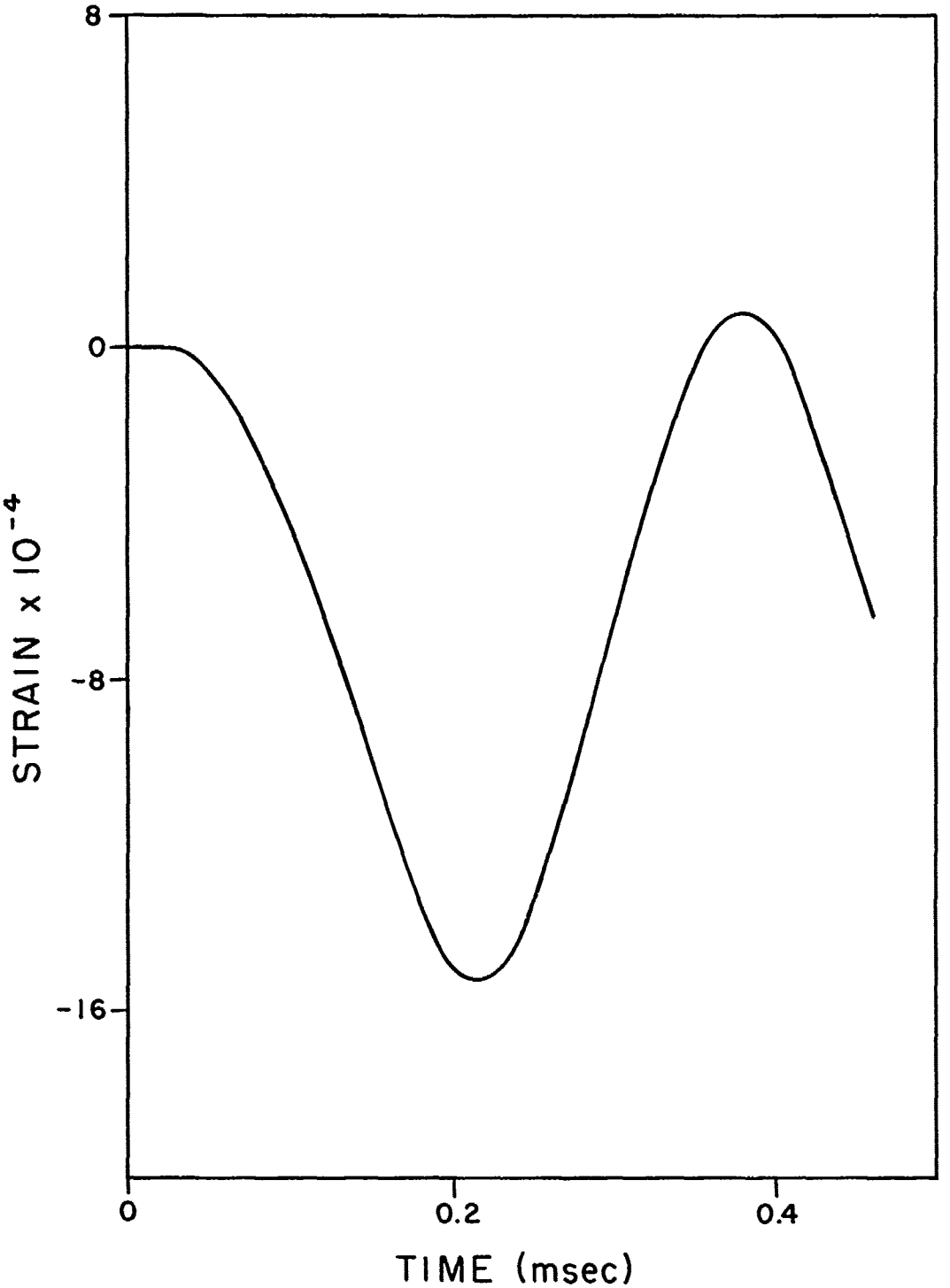

Figure 5. Axial strain at x = 7.0.

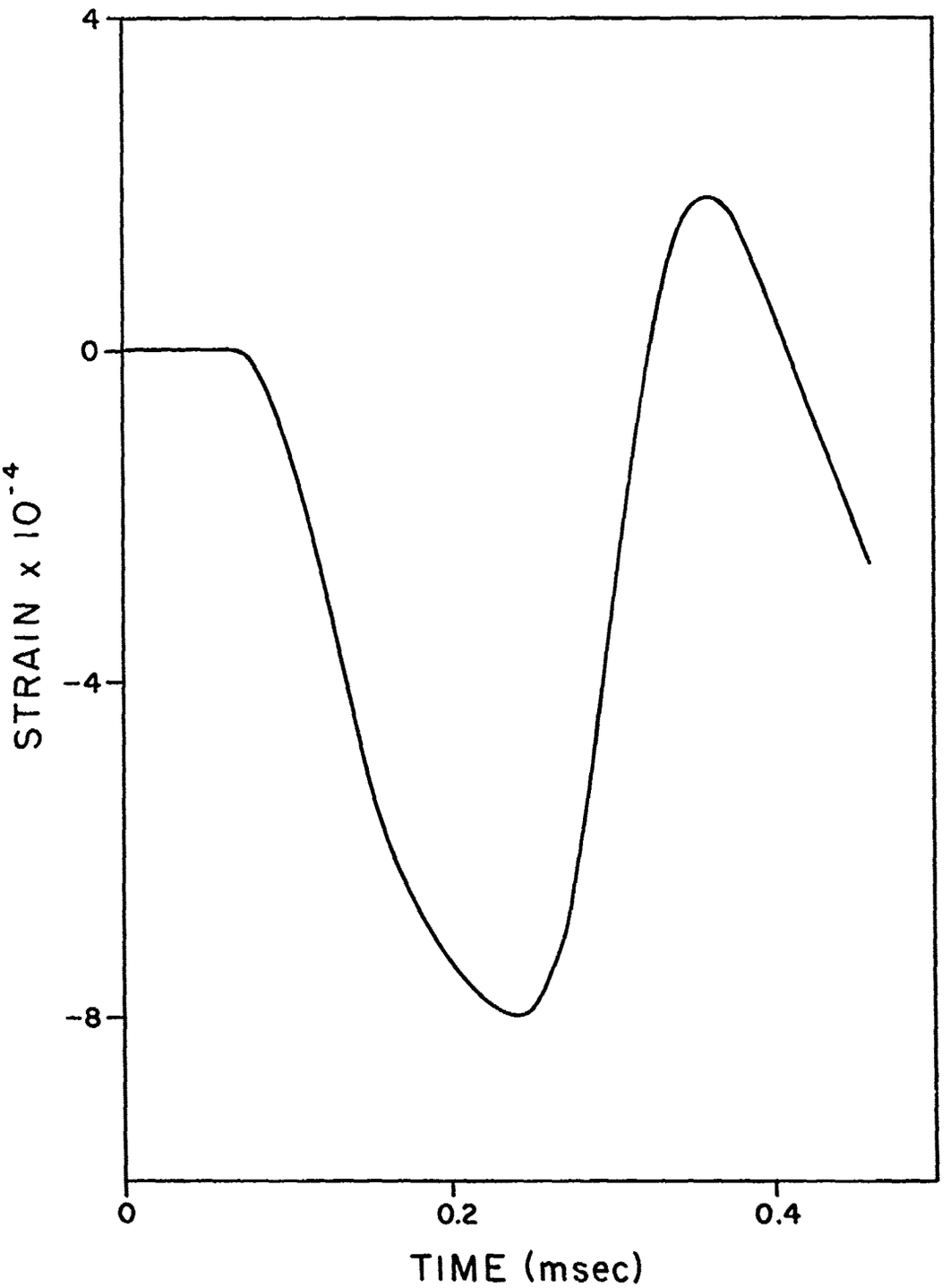

Figure 6. Axial strain at x = 15.0.

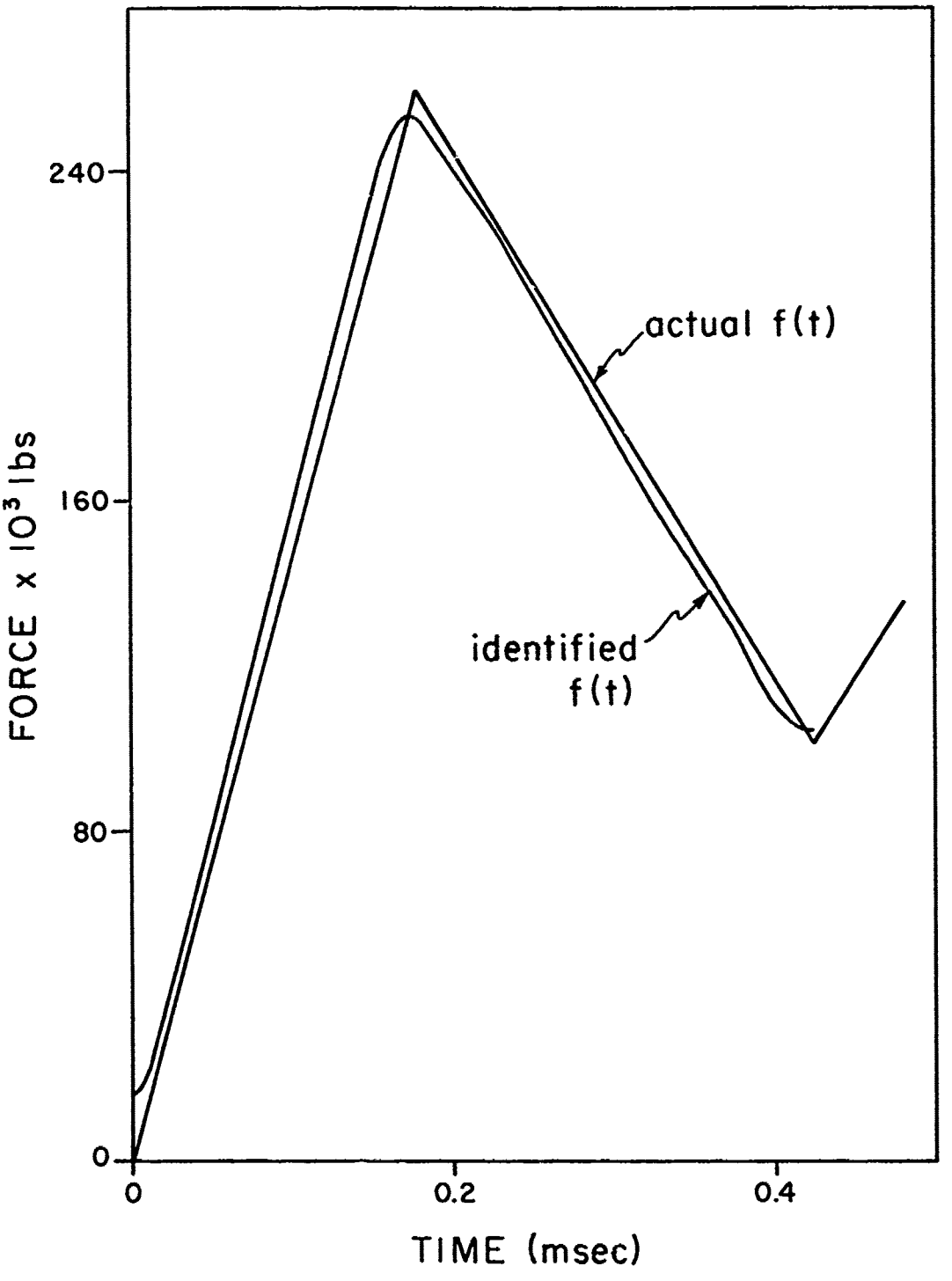

Figure 7. Comparison of actual and identified f(t) using strain at x = 7.0 from analytic solution.

solution. There is a more pronounced oscillation about the actual solution. Some of these oscillations may be removable by digital filtering.

In the third example, a moment with a time history was applied to the nose in addition to an axial force on a finite element model. The identified loads are compared to the applied loads in Fig. 9. In this case, the identification is not as accurate as for the axial force. The use of numerical transforms introduces substantial errors unless tremendous resolution is used in the frequency domain. The identification shown here represents a compromise between adequate resolution and reasonable computer time. The maximum moment and salient aspects of the time history are well represented; but the predicted moment exhibits a significant lag.

Numerical experiments have also been carried out in identifying both the moment and shear from curvature records at two stations. These have been quite unsatisfactory. To obtain a transfer function which is invertible, considerable damping is needed, and the identified forces and moments are quite sensitive to the magnitude of the damping. Therefore, in the following section, only the transverse force was identified for the flexural problem.

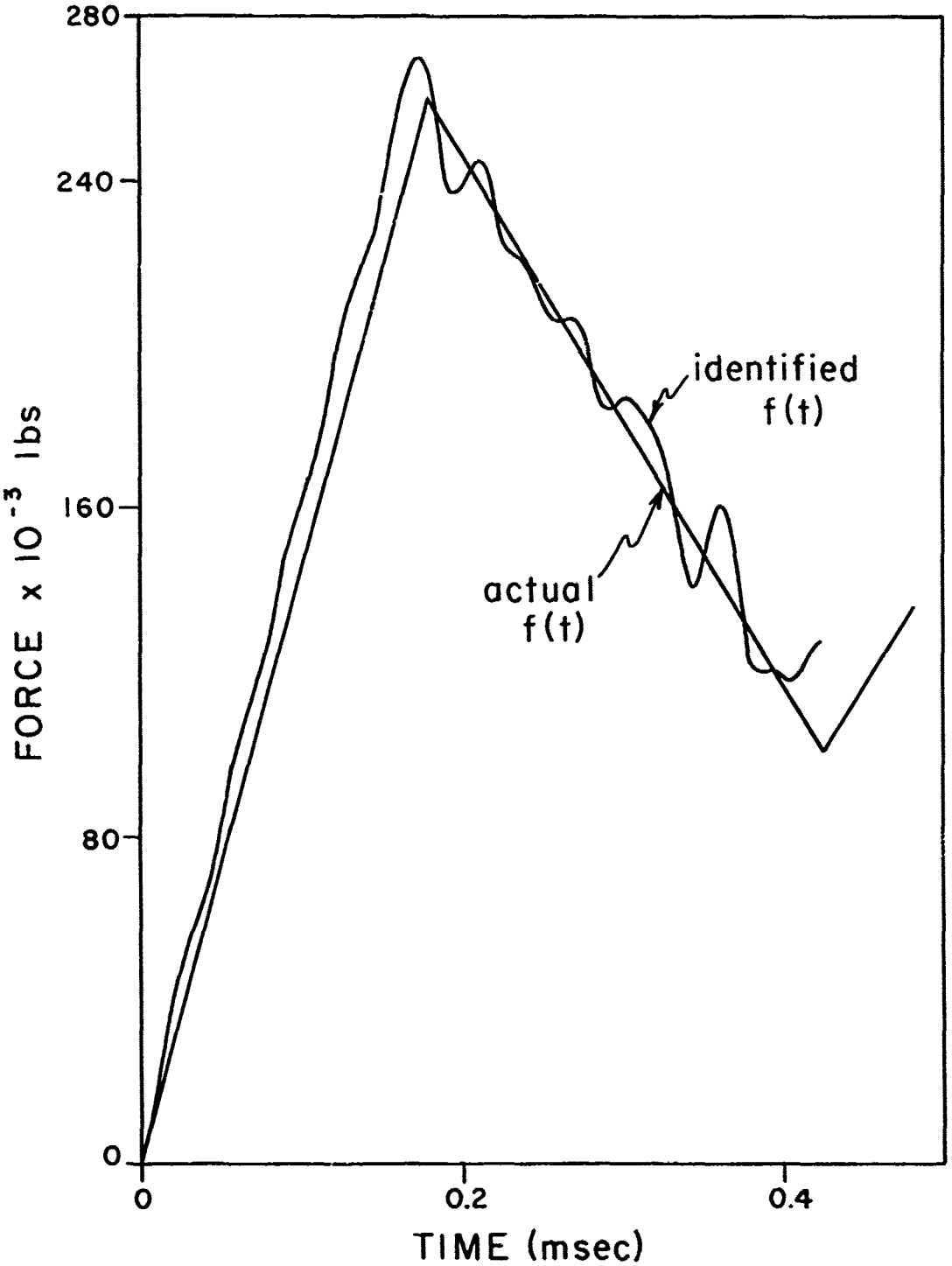

Figure 8. Comparison of actual and identified f(t) using strain at x = 7.0 from finite element solution.

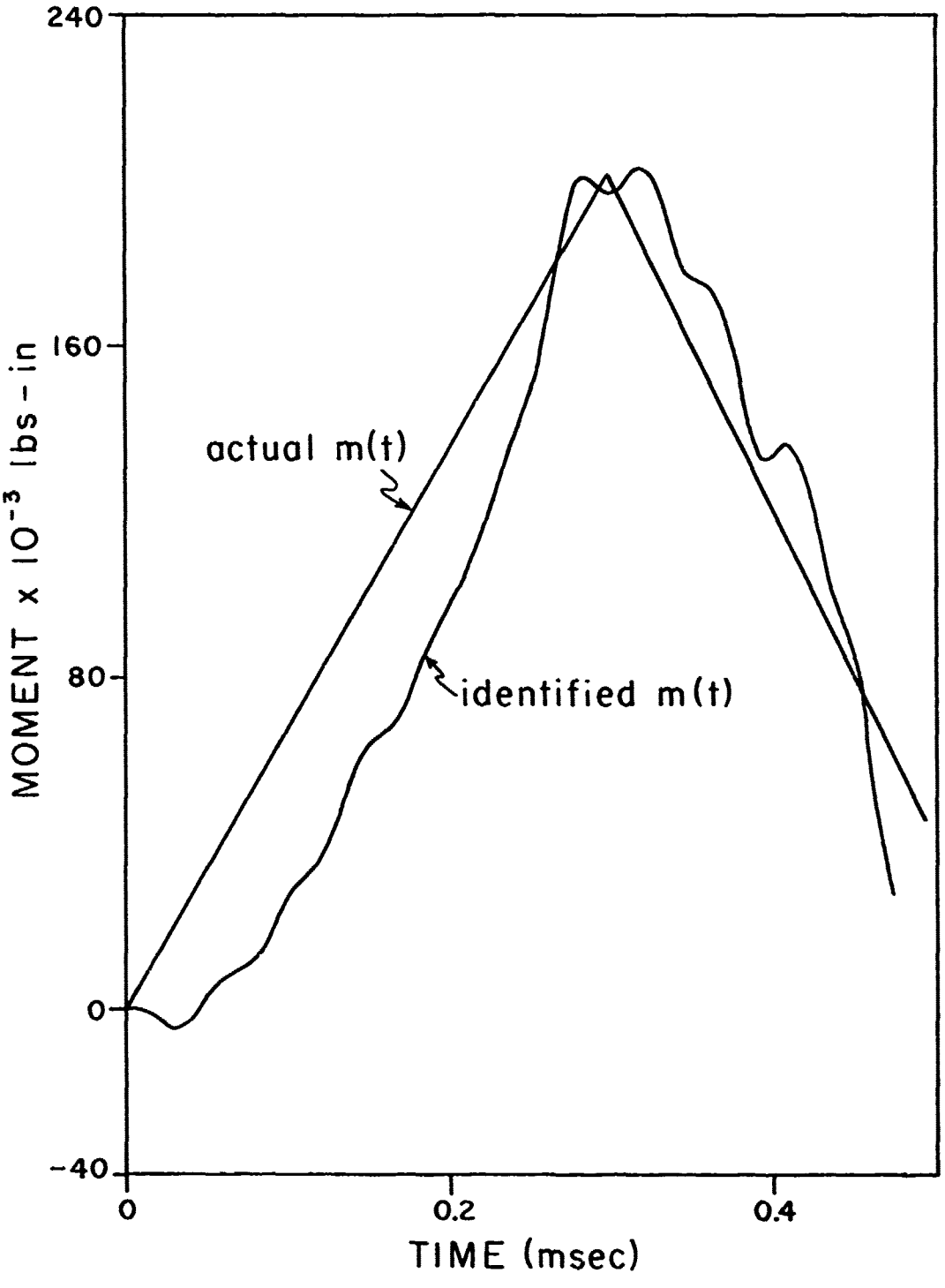

Figure 9. Comparison of actual and identified moment using strain from finite element solution.

SECTION VI

LOADS FOR DNA REVERSE BALLISTIC EXPERIMENTS

We will here describe the loads identified for the DNA reverse ballistic experiments conducted at Sandia Laboratories (ref. 1). The study is limited to Test 3 in which the projectile was in a 3 degree nose-down attitude; i.e. the angle of attack was 3 degrees. Test data consisted of four accelerometer records, two axial and two lateral, and seventeen axial strain gauges.

In this Section, we will describe the simplifications which were necessary to generate a model suitable for the force identification. Once the forces were identified, they were applied to a detailed finite element model of the projectile. The strains and accelerations predicted by the finite element model are then compared to experimental results.

A schematic of the projectile is shown in Fig. 10. The idealization employed for the force identification is shown in Fig. 11. Several features of the projectile had to be omitted because the identification model is limited to a single rigid mass and a rod of uniform properties. The rigid mass was used to model the portion of the projectile between 0 and 3.45 inches. The uniform rod was then given the dimensions of an average cross-section. In the actual model, we have four distinct sections behind the nose (1) the kennertium plug and steel barrel from 3.45 inches to 7.45 inches; (2) the 1.702 inch O.D. section from 7.45 inches to 9.64 that houses the front accelerometers; (3) the tapered section from 9.64 inches to 13.04 inches, in which the O.D. increases from 1.702 inches to 1.900 inches; (4) the last constant diameter section from 13.045 inches to 18.15 inches. The idealized model is too stiff in comparison to the first half of the vehicle, and too

flexible in comparison to the second half.

The loads were identified from the strain gauge records at station 9.6 inches, gauges 3 and 10. (shown in Figs. 17 and 18). This location was chosen because it is as far as possible from the irregularities near the front accelerometer and relatively clean records were obtained in Test 3. The force was identified only for 0.4 msec; after that time the vehicle penetrates beyond the nose.

The identified axial and transverse loads are shown in Fig. 12. The maximum axial load is 130,000 lbs. and occurs at 300 microseconds; the maximum transverse load is 26,000 lbs. and occurs at 50 microseconds. Both of the records shown were extensively filtered.

These loads were then applied to the finite element model shown in Fig. 11 for a 0.6 msec simulation, the loads at 0.4 msec were held constant. The model was solved by the program WHAMS - 2D (ref. 4) using explicit time integration. All acceleration results were smoothed by a 10 point averaging filter (ref. 5). The acceleration results are compared to the four accelerometer records for Test 3 in Figs. 13 to 16. As can be seen, the axial accelerations, Figs. 13 and 14, agree quite well with the experiment, indicating that the axial load identification was successful. The agreement of the lateral records, Figs. 15 and 16, is quite poor.

Strain gauge output is compared to the experiment in Figs. 17 to 23. Particularly for the first 0.4 msec, the agreement is satisfactory. The increasing discrepancy after this time is understandable since the loads were only identified to 0.4 msec. However, it is unclear why the agreement in lateral accelerations is so poor in comparison to the strains. A possible explanation may lie in the nonuniqueness of the identification problem. If a different model were selected, the nonuniqueness may lead to substantially different lateral forces but still the same strains. It is this nonuniqueness which is also undoubtedly related to the numerical difficulties of inverting the problem.

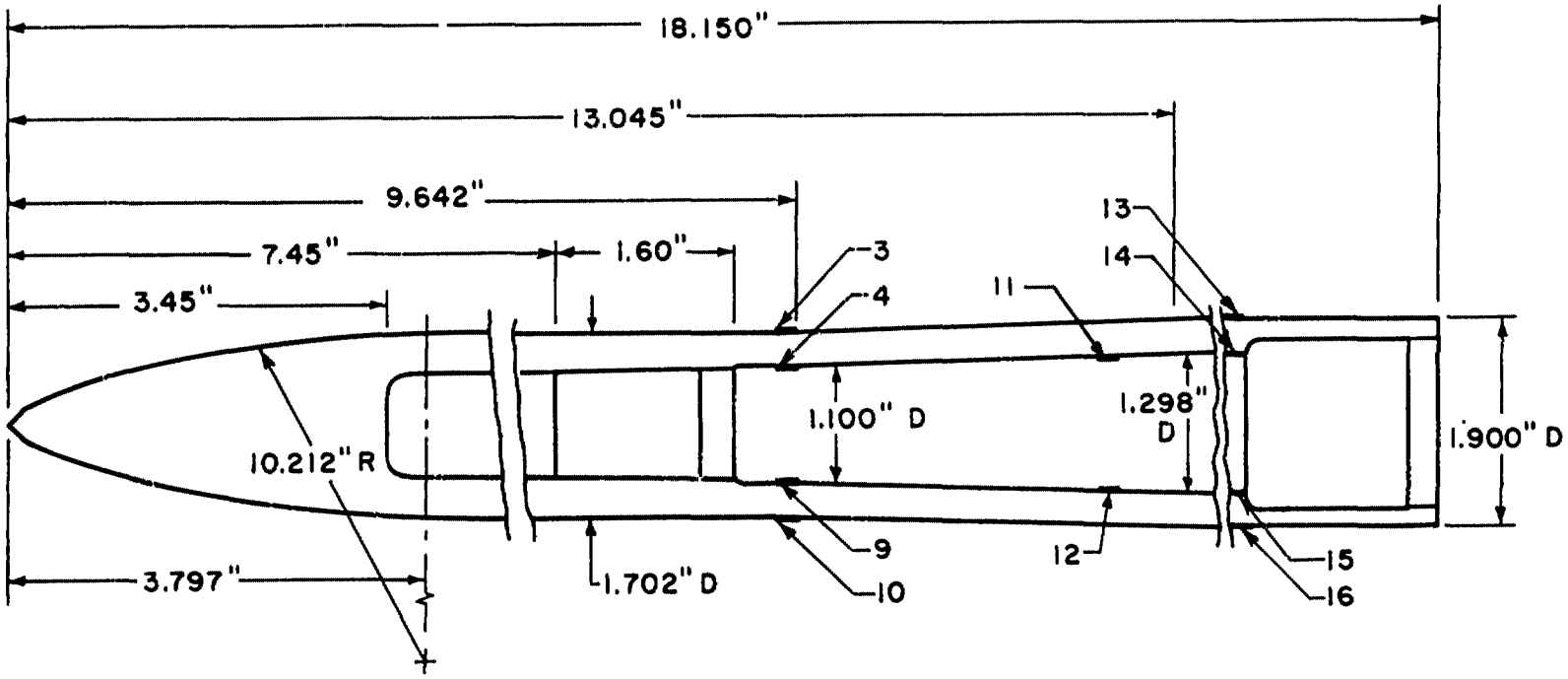

Figure 10. DNA-SANDIA vehicle employed in reverse ballistic test.

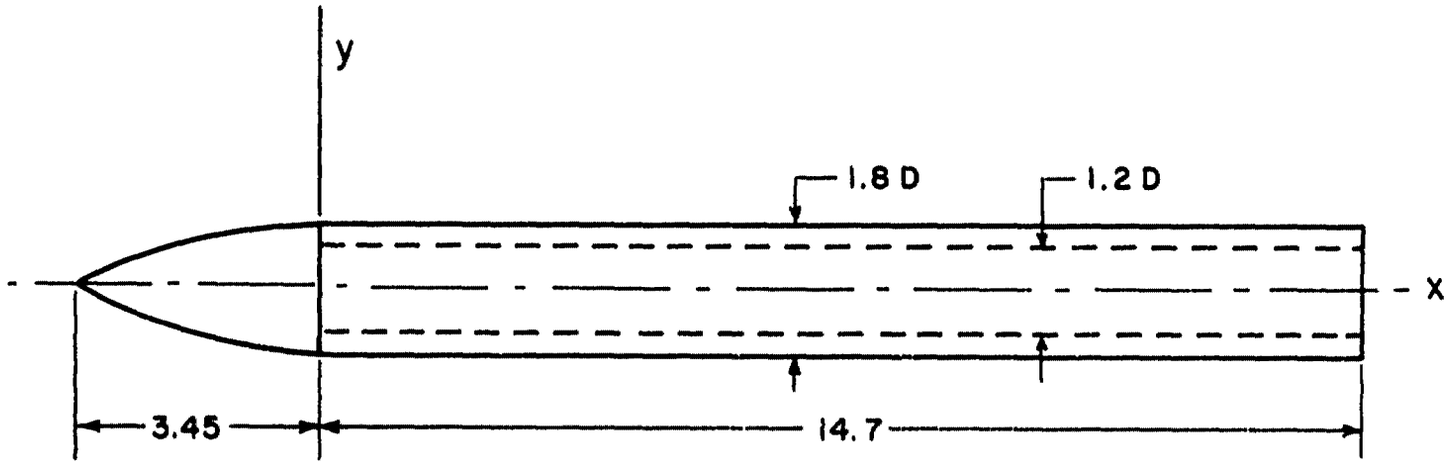

IDENTIFICATION MODEL

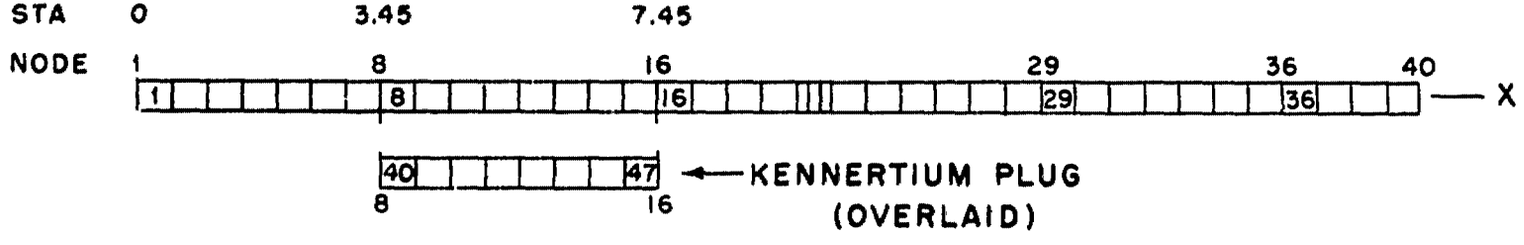

FINITE ELEMENT MODEL

Figure 11. Idealization of DNA-SANDIA vehicle for identification problem and finite element model for calculation of response from identical force.

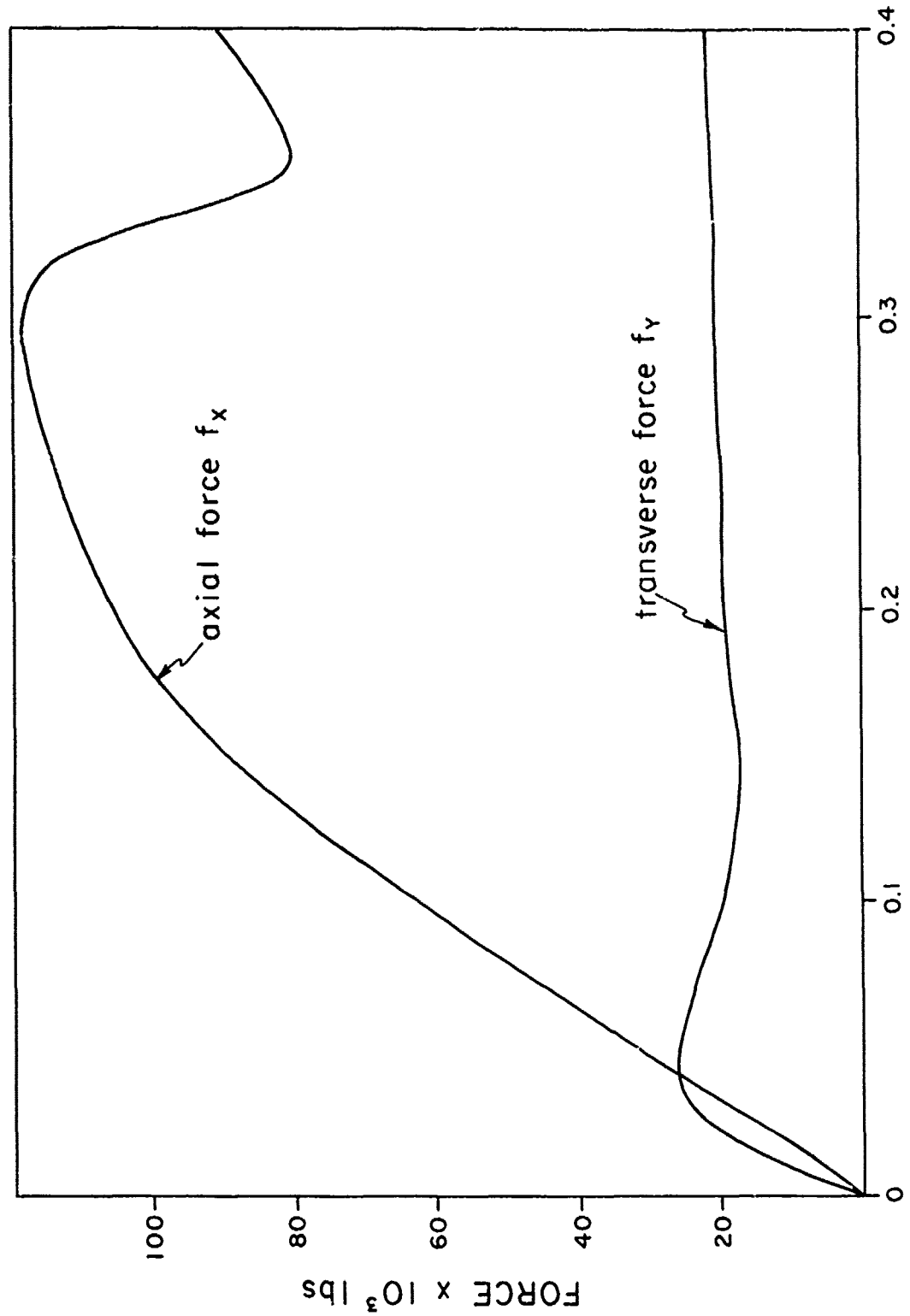

Figure 12. Forces identified on nose.

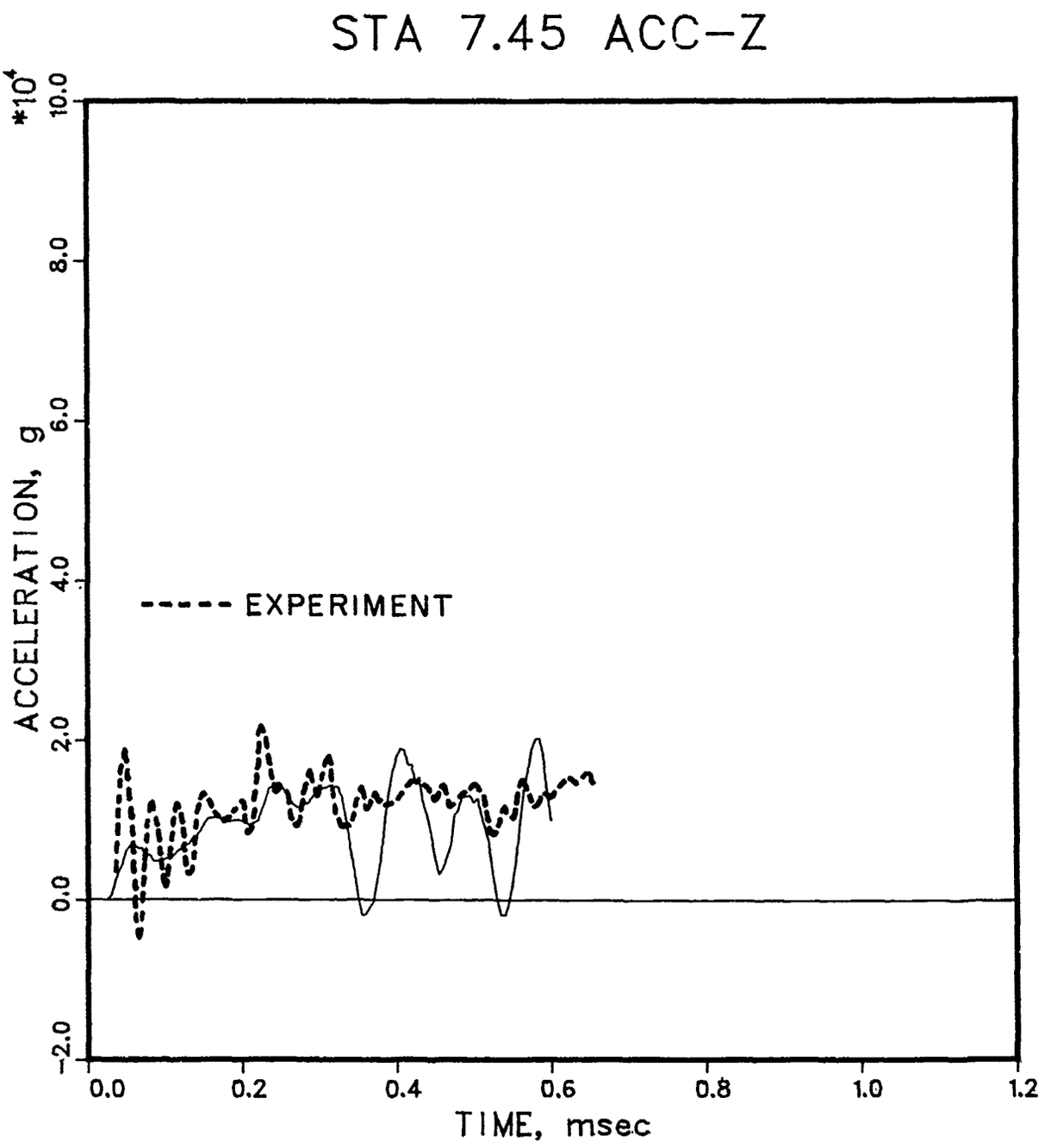

Figure 13. Axial acceleration (x-component) at station 7.45 (Accelerometer 2)

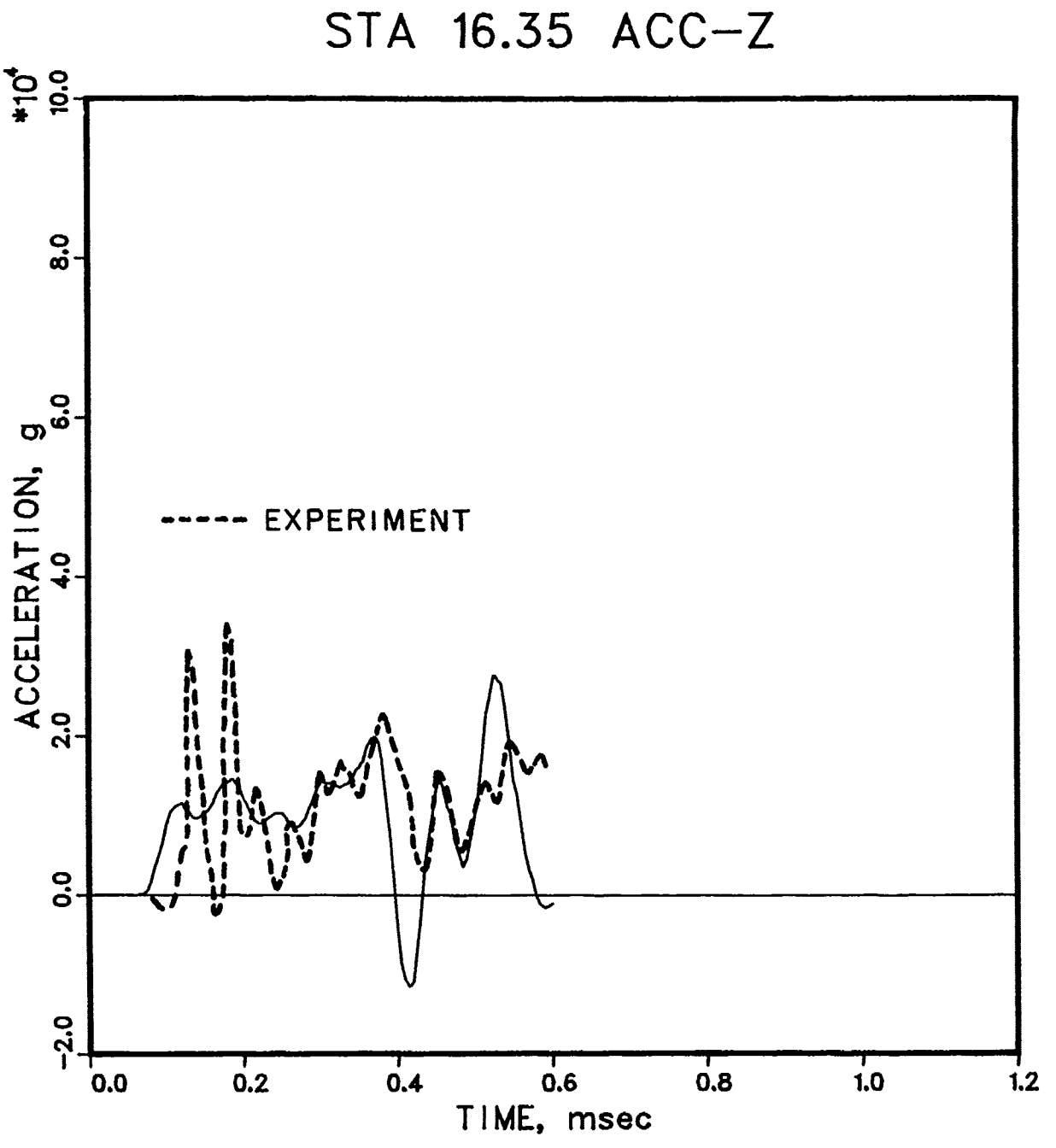

Figure 14. Axial acceleration (x-component) at station 16.35 (Accelerometer 4)

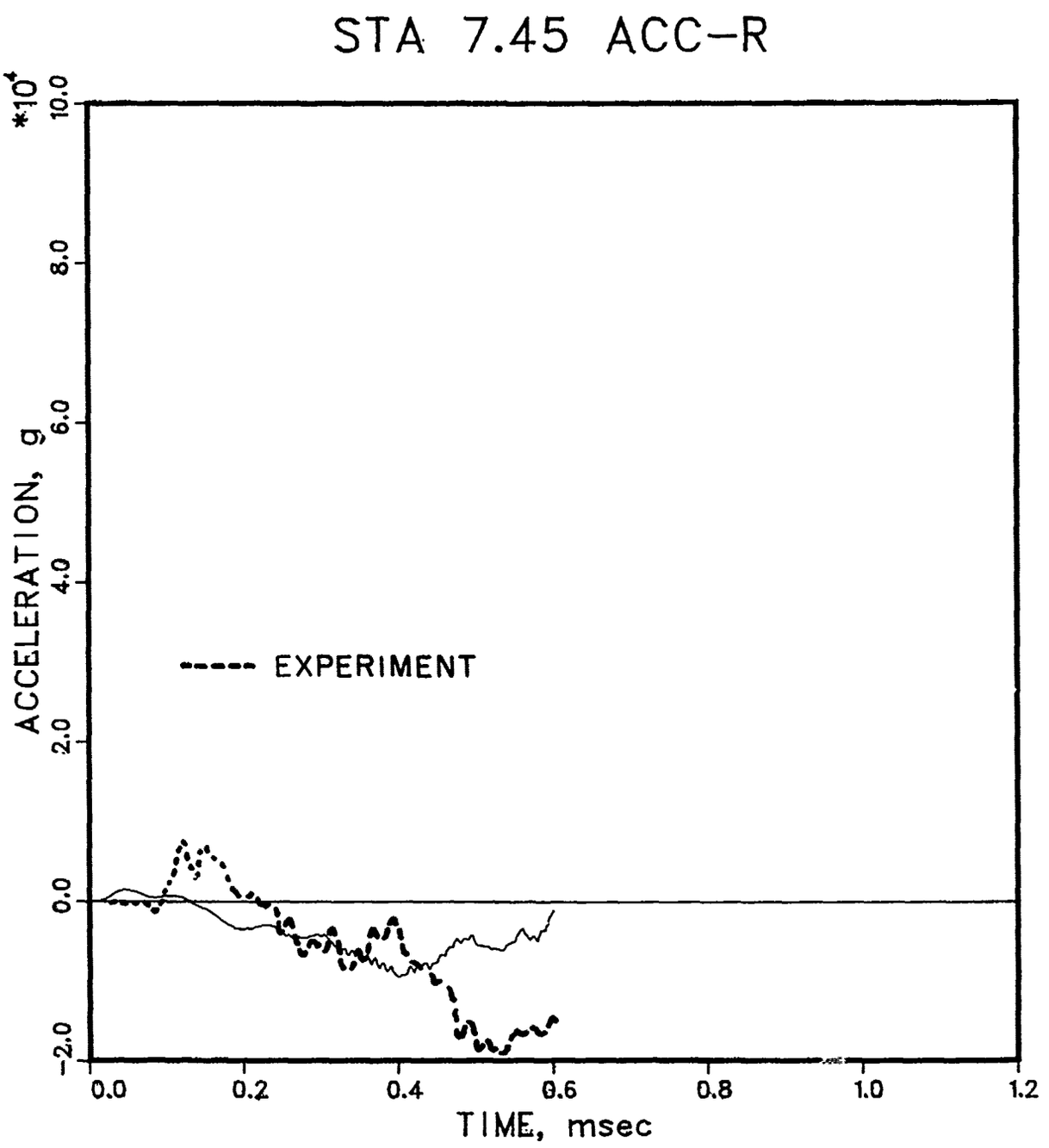

Figure 15. Lateral acceleration (y-component) at station 7.45 (Accelerometer 1)

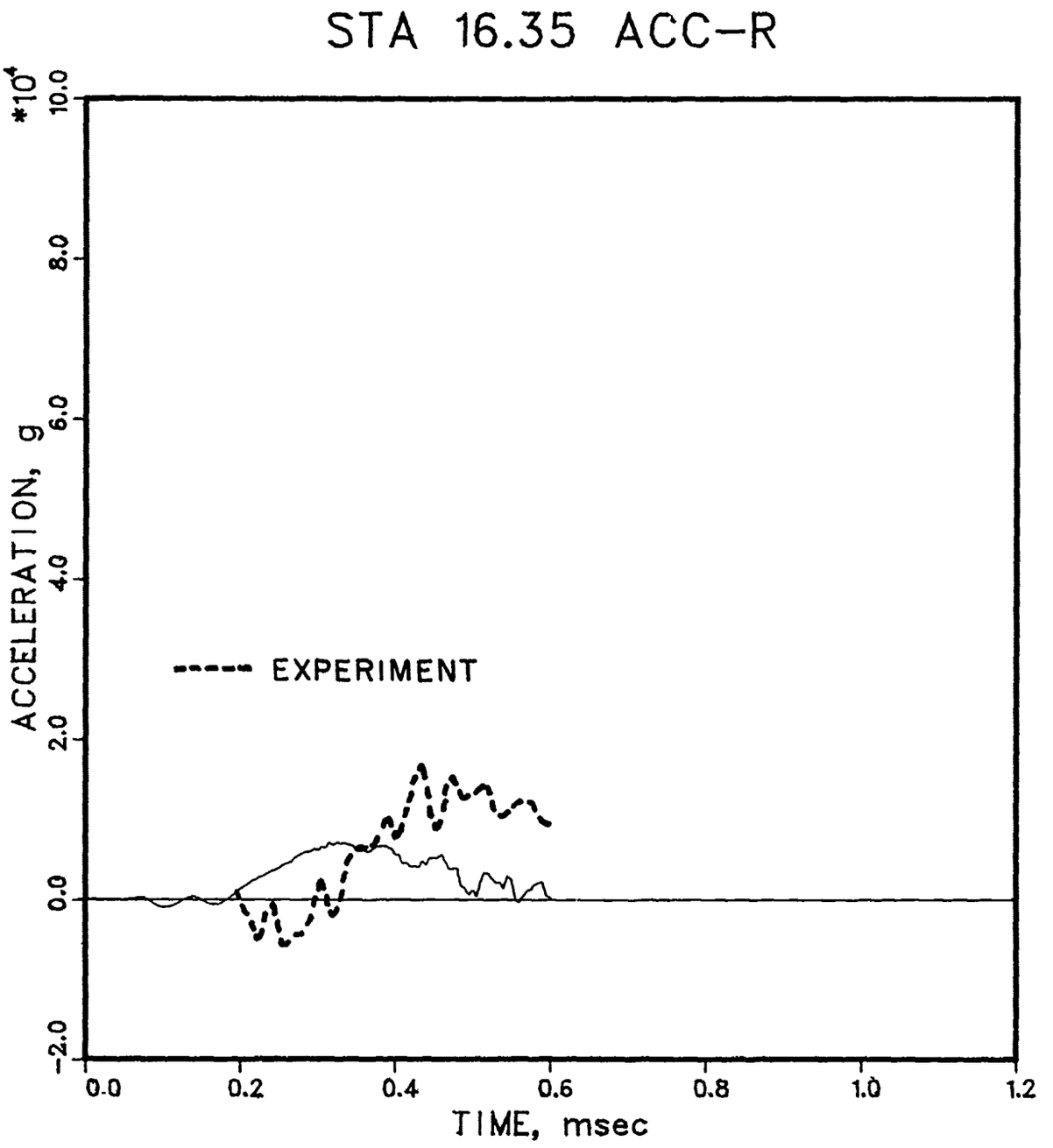

Figure 16. Lateral acceleration (y-component) at station 16.35 (Accelerometer 3)

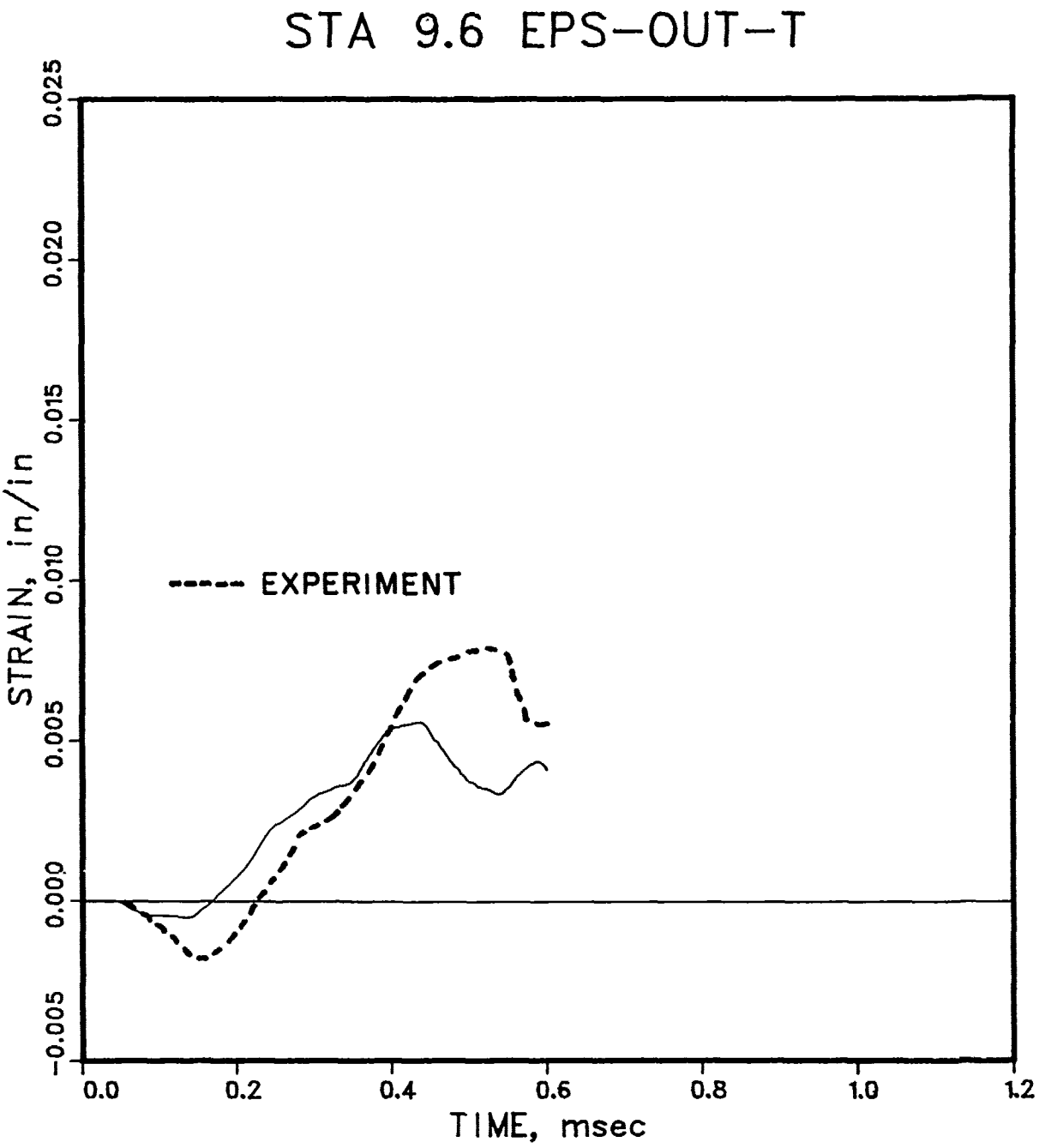

Figure 17. Strain (outside top) at station 9.6 (Strain gauge 3)

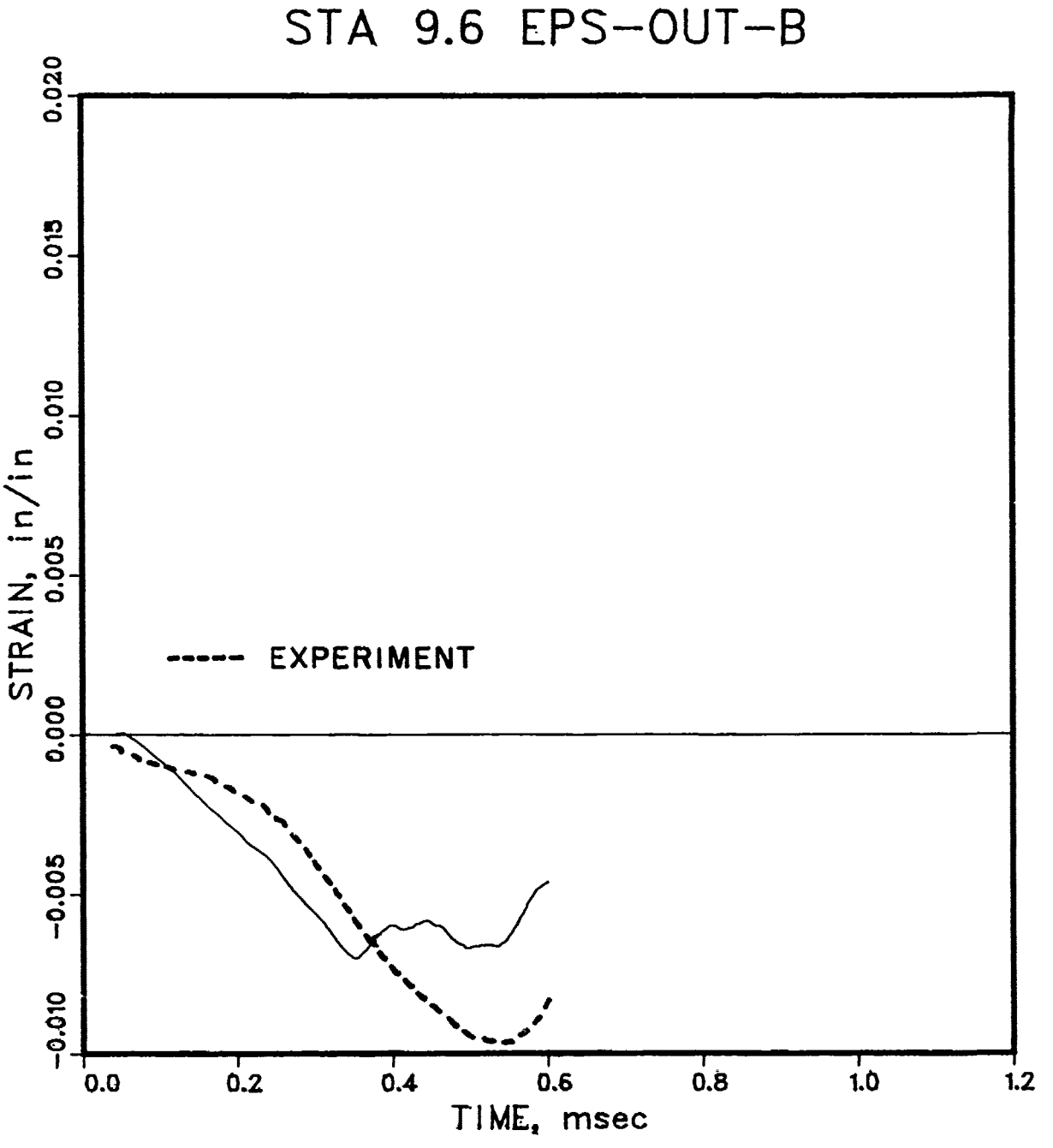

Figure 18. Strain (outside bottom) at station 9.6 (Strain gauge 10)

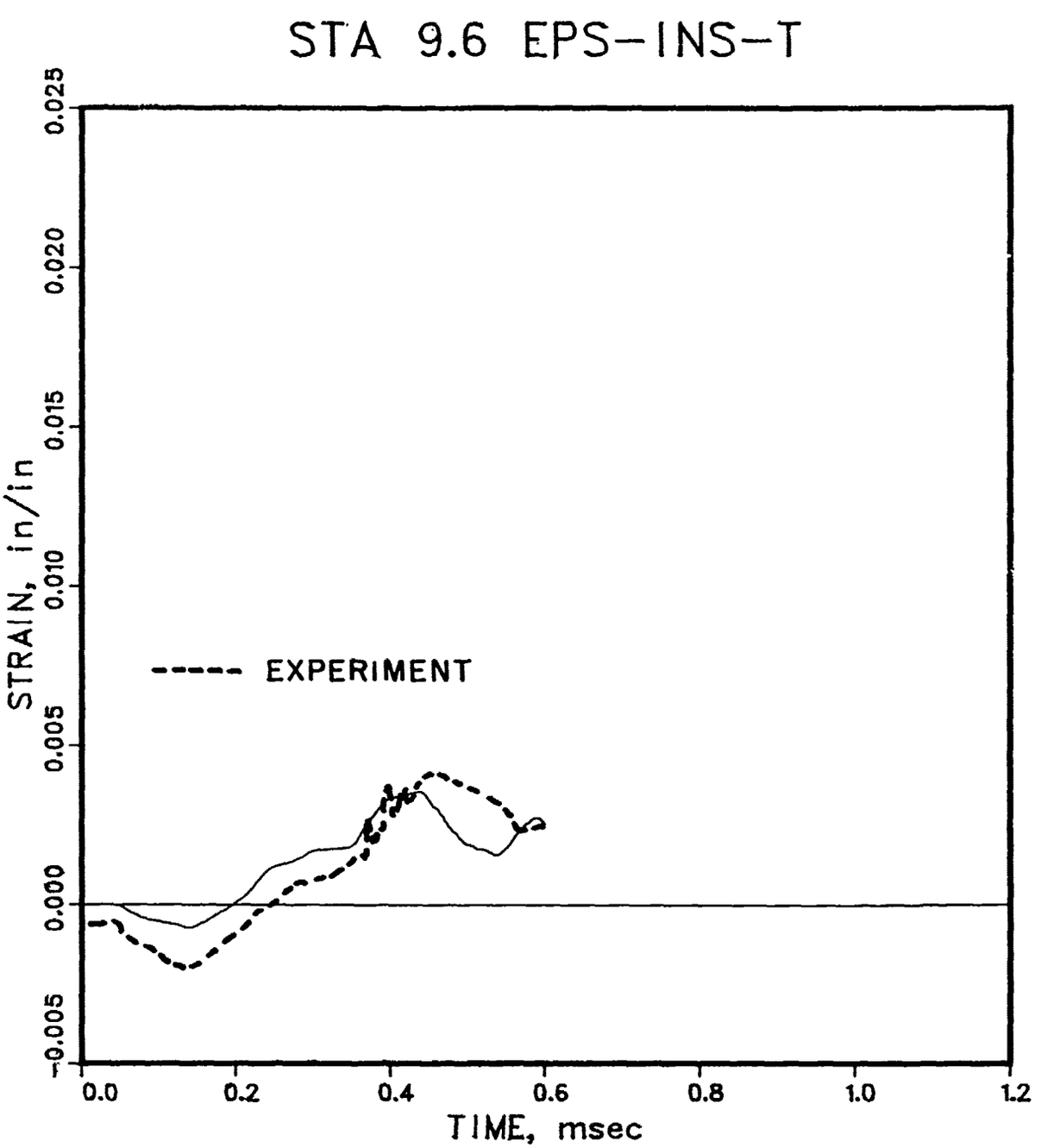

Figure 19. Strain (inside top) at station 9.6 (Strain gauge 4)

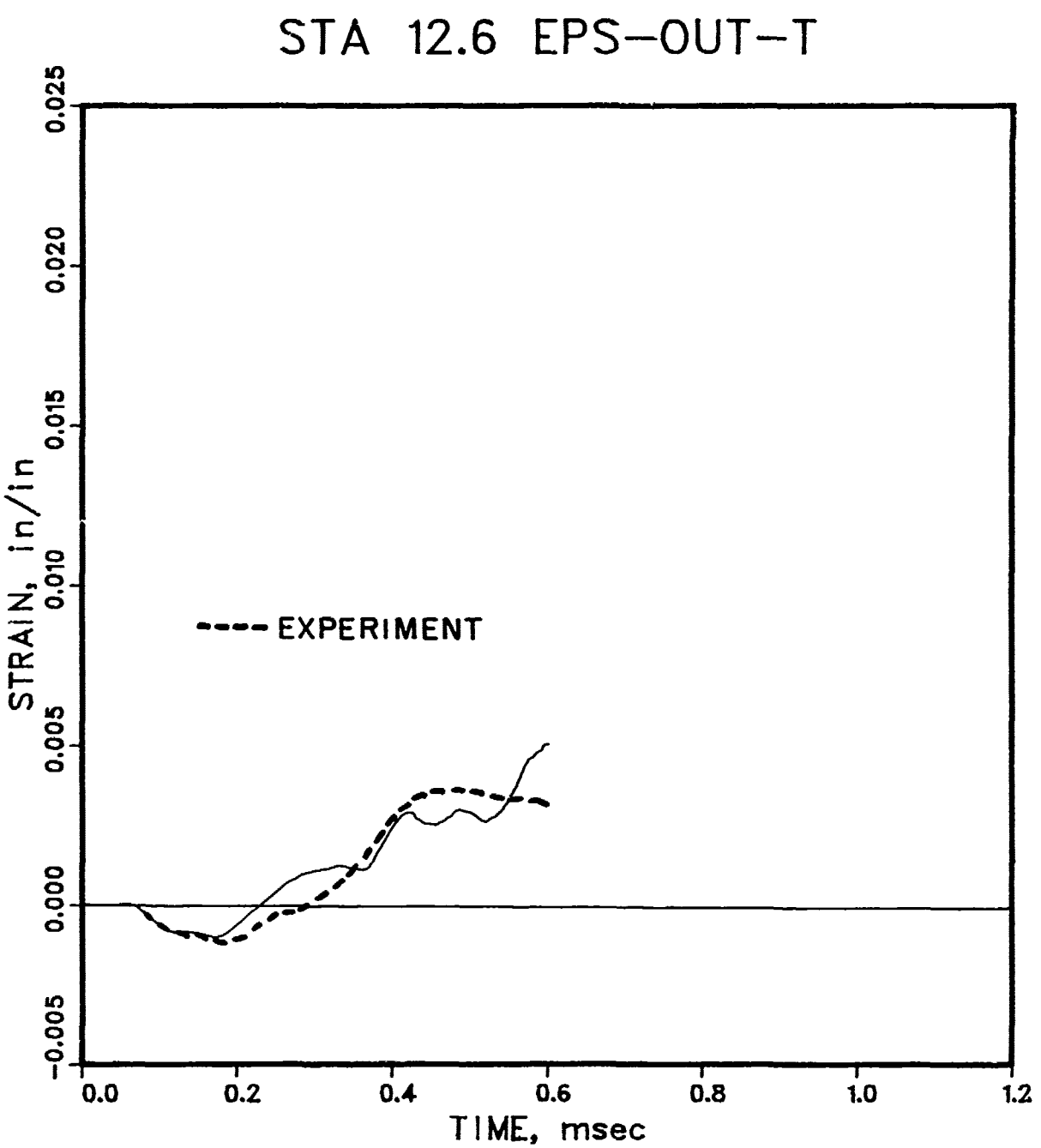

Figure 20. Strain (outside top) at station 12.6 (Strain gauge 11)

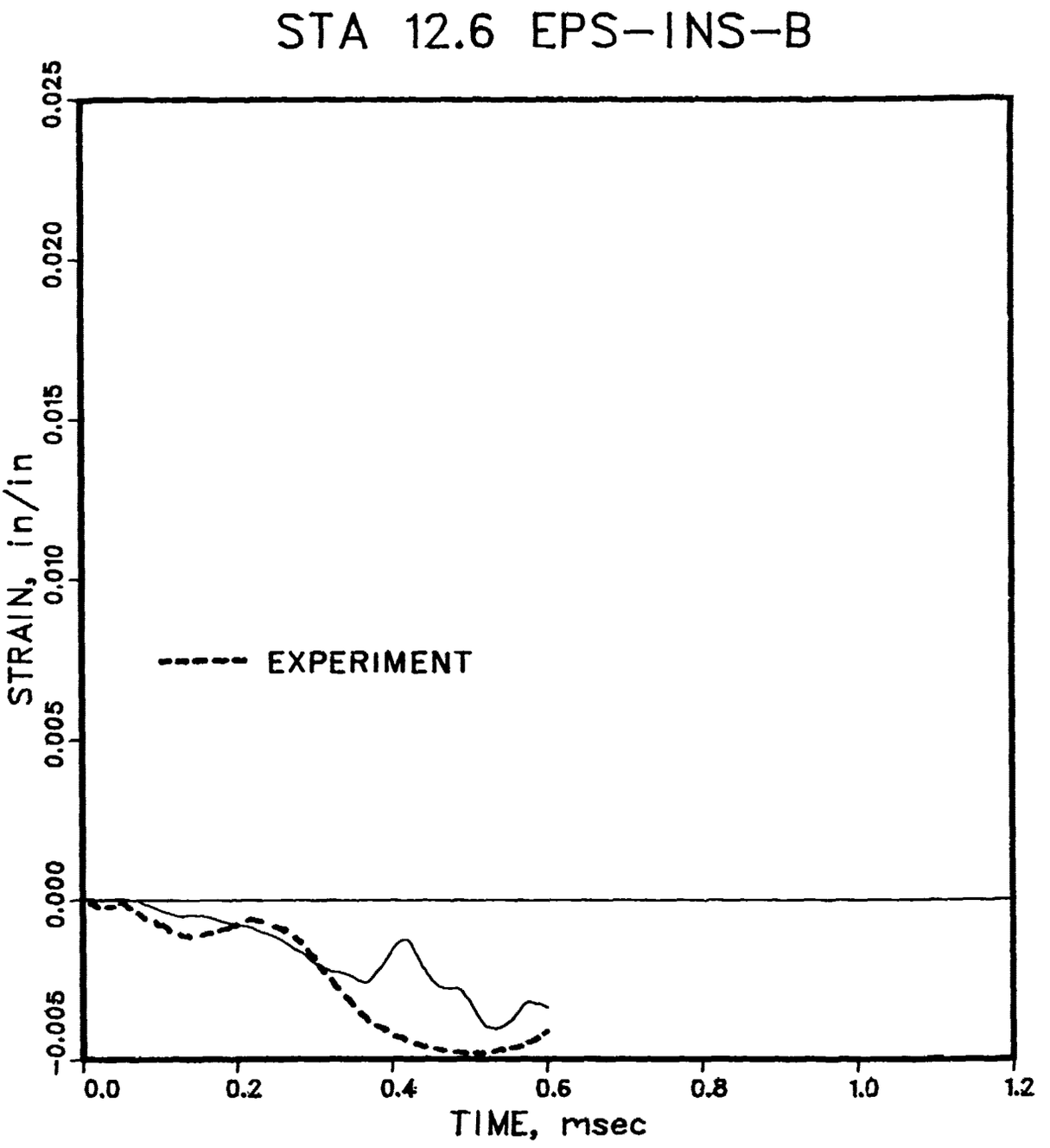

Figure 21. Strain (inside bottom) at station 12.6 (Strain gauge 12)

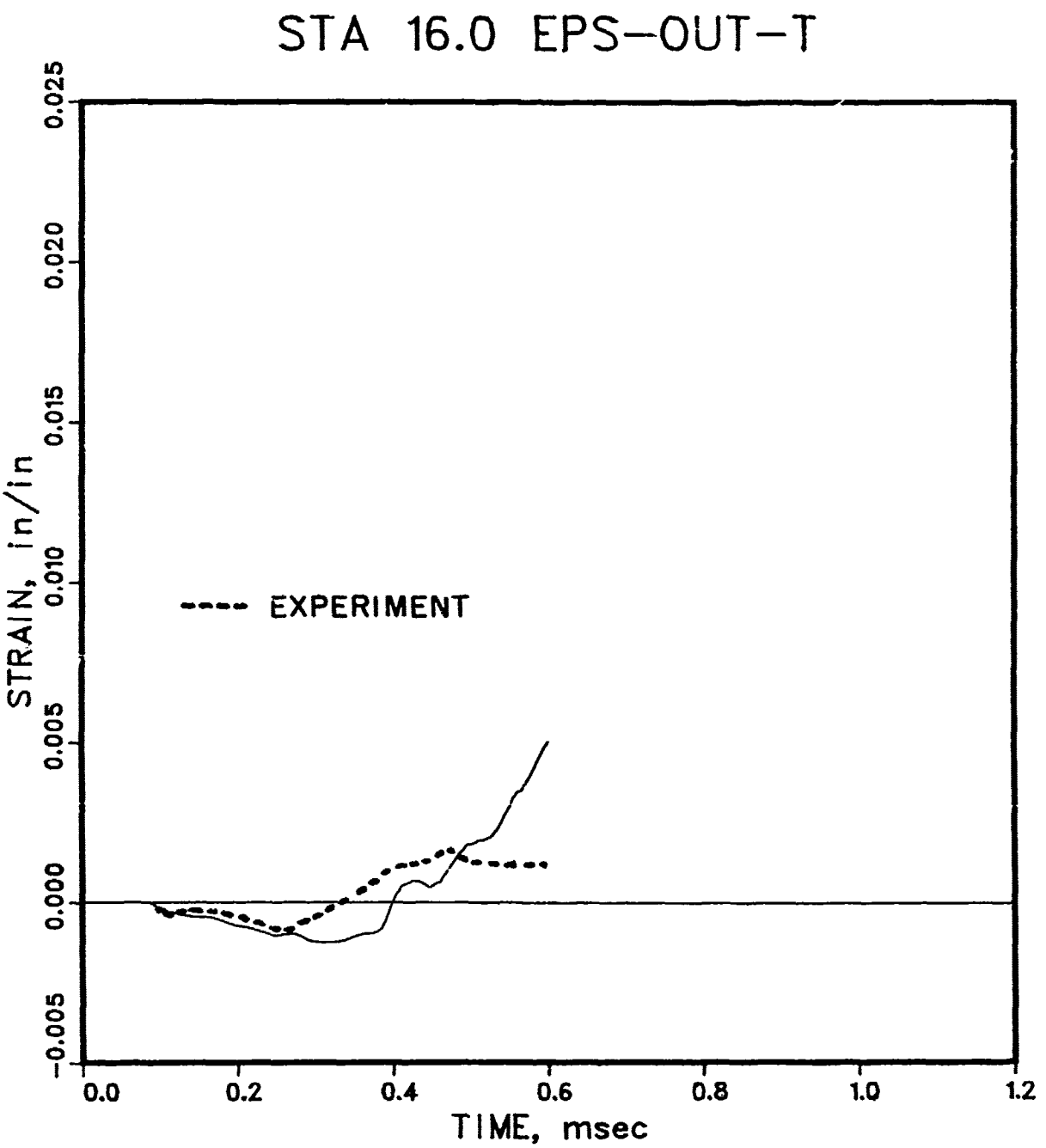

Figure 22. Strain (outside top) at station 16 (Strain gauge 13)

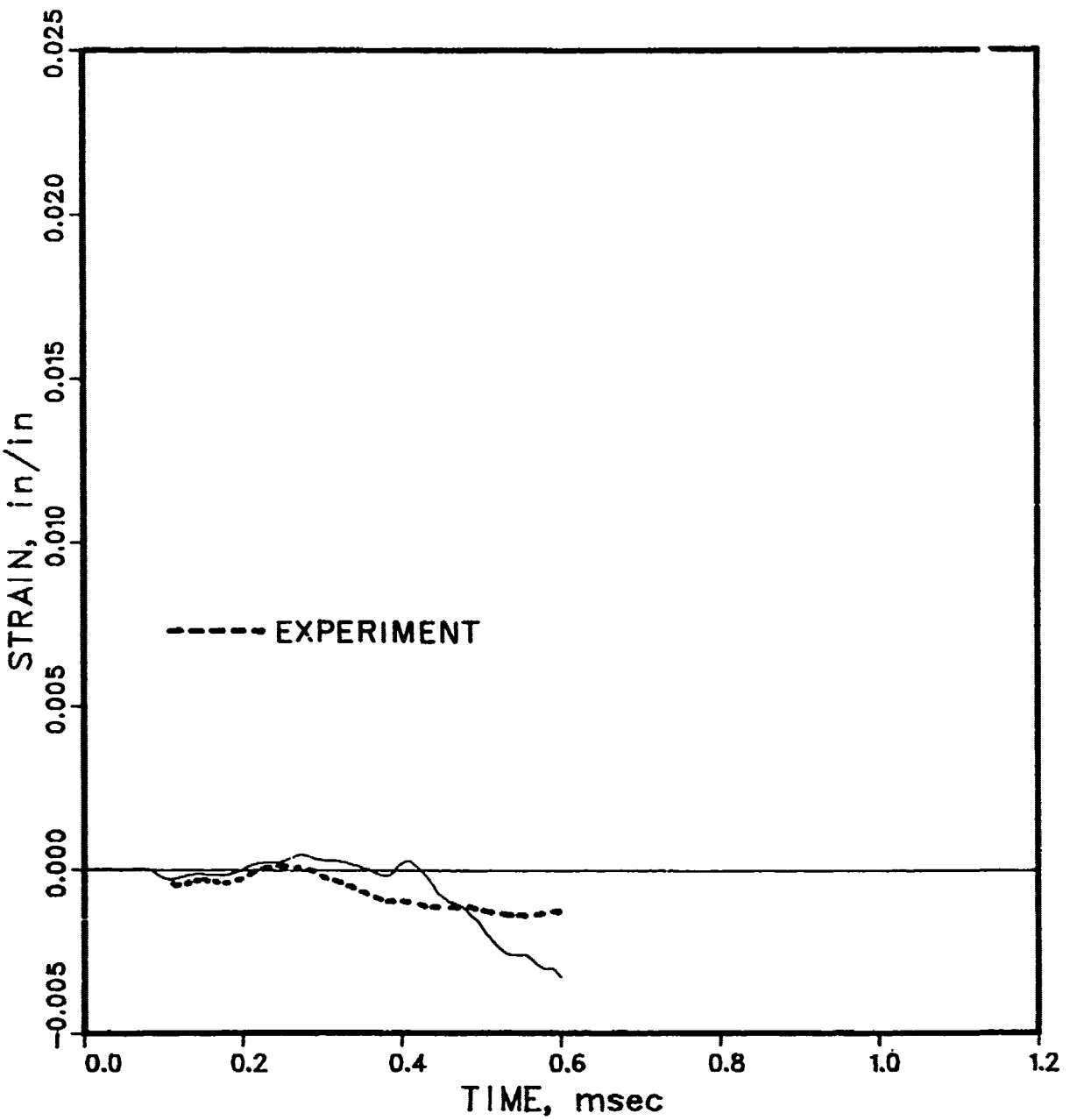

Figure 23. Strain (inside bottom) at station 16 (Strain gauge 15)

REFERENCES

1. Creighton, D.C. "Correlation of Additional Reverse Ballistic Test Data", U.S. Army Waterways Experiment Station Report on Work Unit 18, Subtask SB211, for DNA, August 1978.

2. Wagner, M.H., Fulton, C.C. and Goerke, S.W., "Calculation of Reverse Ballistic Test into Dakota Sandstone at 1800 Ft./sec.", California Research and Technology, Contract DNA001-76-C-0157, February 1976.

3. Belytschko, T.B., "Semianalytic Methods for Axial Response Analysis of Penetrators," DNA Report, DNA 4044F, June 1976.

4. Belytschko, T.B. and Mullen, R.M. "WHAMS, A Program for the Transient Analysis of Structures and Continua", Structural Mechanics Software Series, ed. by N. Perrone and W. Pilkey, Vol. 2, University Press of Virginia, pp. 151-212, 1978.

5. Holmes, N. and Belytschko, T.B., "Postprocessing of Finite Element Transient Response Calculations by Digital Filters", Computers and Structures, Vol. 6, 211-216, 1976.

DISTRIBUTION LIST

DEPARTMENT OF DEFENSE

Assistant to the Secretary of Defense
Atomic Energy
ATTN: Executive Assistant

Defense Advanced Rsch Proj Agency
ATTN: TIO

Defense Intelligence Agency
ATTN: DB-4N
ATTN: DB-4C, E. O'Farrell
ATTN: DT-2
ATTN: RDS-3A

Defense Nuclear Agency
ATTN: SPAS
4 cy ATTN: TITL
5 cy ATTN: SPSS

Defense Technical Information Center
12 cy ATTN: DD

Field Command
Defense Nuclear Agency
ATTN: FCPR

Field Command
Defense Nuclear Agency
Livermore Branch
ATTN: FCPRL

Interservice Nuclear Weapons School
ATTN: TTV

Joint Strat Tgt Planning Staff
ATTN: JLA
ATTN: NRI-STINFO Library

NATO School (SHAPE)
ATTN: U.S. Documents Officer

Undersecretary of Def for Rsch & Engrg
ATTN: Strategic & Space Systems (OS)

DEPARTMENT OF THE ARMY

Chief of Engineers
Department of the Army
2 cy ATTN: DAEN-MCE-D
2 cy ATTN: DAEN-RDL

Deputy Chief of Staff for Ops & Plans
Department of the Army
ATTN: DAMO-NC

Deputy Chief of Staff for Rsch Dev & Acq
Department of the Army
ATTN: DAMA-CSS-N, N. Barron

Engineer Studies Center
Department of the Army
ATTN: DAEN-FES

Gator Mine Program
Department of the Army
ATTN: E. Lindsey

DEPARTMENT OF THE ARMY (Continued)

Harry Diamond Laboratories
Department of the Army
ATTN: DELHD-N-P
ATTN: DELHD-N-P, J. Gualtney

U.S. Army Armament Material Readiness Cmd
ATTN: MA Library

U.S. Army Ballistic Research Labs
ATTN: DRDAR-BLT
ATTN: DRDAR-BLT, G. Grabarek
ATTN: DRDAR-BLT, J. Keefer
ATTN: DRDAR-BLT, A. Ricchiazzi
ATTN: DRDAR-BL
ATTN: DRDAR-BLT, G. Roecker
2 cy ATTN: DRDAR-TSB-S

U.S. Army Cold Region Res Engr Lab
ATTN: G. Swinzow

U.S. Army Concepts Analysis Agency
ATTN: CSSA-ADL

U.S. Army Engineer Center
ATTN: ATZA

U.S. Army Engineer Div Huntsville
ATTN: HNDED-SR

U.S. Army Engineer Div Missouri River
ATTN: Technical Library

U.S. Army Engineer School
ATTN: ATZA-DTE-ADM
ATTN: ATZA-CDC

U.S. Army Engr Waterways Exper Station
ATTN: J. Strange
ATTN: D. Butler
ATTN: WESSD, J. Jackson
ATTN: B. Rohani
ATTN: WESSE, L. Ingram
ATTN: Library
ATTN: WESSA, W. Flathau

U.S. Army Mat Cmd Proj Mngr for Nuc Munitions
ATTN: DRCPM-NUC

U.S. Army Material & Mechanics Rsch Ctr
ATTN: Technical Library

U.S. Army Materiel Dev & Readiness Cmd
ATTN: DRXAM-TL

U.S. Army Materiel Sys Analysis Activity
ATTN: DRXSY-D, J. Sperrazza

U.S. Army Missile R&D Command
ATTN: RSIC
ATTN: F. Fleming
ATTN: DRCPM-PE, W. Jann

U.S. Army Mobility Equip R&D Cmd
ATTN: DRDME-WC
ATTN: DRDME-XS

DEPARTMENT OF THE ARMY (Continued)

U.S. Army Nuclear & Chemical Agency
ATTN: Library

U.S. Army War College
ATTN: Library

DEPARTMENT OF THE NAVY

Marine Corps
Department of the Navy
ATTN: POM

Marine Corp Dev & Education Command
Fire Support Section
Department of the Navy
ATTN: D091, J. Hartneady

Naval Construction Battalion Center
ATTN: Code L08A
ATTN: Code L51, R. Odello

Naval Explosive Ord Disposal Fac
ATTN: Code 504, J. Petrousky

Naval Postgraduate School
ATTN: Code 1424 Library

Naval Research Laboratory
ATTN: Code 2627

Naval Sea Systems Command
ATTN: SEA-9931G
ATTN: SEA-033

Naval Surface Weapons Center
White Oak Laboratory
ATTN: Code U401, M. Kleinerman
ATTN: Code F31
ATTN: Code X211

Naval Surface Weapons Center
ATTN: Tech Library & Info Svcs Branch

Naval Weapons Center
ATTN: Code 266, C. Austin
ATTN: Code 233

Naval Weapons Evaluation Facility
ATTN: Code 10

Office of the Chief of Naval Operations
ATTN: OP 982
ATTN: OP 654C3, R. Piacesi
ATTN: OP 982E, M. Lenzini

Strategic Systems Project Office
Department of the Navy
ATTN: NSP-43

DEPARTMENT OF THE AIR FORCE

Air Force Armament Laboratory
ATTN: ADTC/XRS, M. Valentine
3 cy ATTN: DLIV, J. Collins

Air Force Institute of Technology
ATTN: Library

DEPARTMENT OF THE AIR FORCE (Continued)

Air Force Weapons Laboratory
Air Force Systems Command
ATTN: SUL

Assistant Chief of Staff
Intelligence
Department of the Air Force
ATTN: INT

Strategic Air Command/INT
Department of the Air Force
ATTN: J. McKinney

Deputy Chief of Staff
Research, Development, & Acq
Department of the Air Force
ATTN: R. Steere

Foreign Technology Division
Air Force Systems Command
ATTN: NIIS Library

Headquarters Space Division
Air Force Systems Command
ATTN: RSS

Oklahoma State University
Fld Off for Wpns Effectiveness
Department of the Air Force
ATTN: E. Jackett

Rome Air Development Center
Air Force Systems Command
ATTN: TSLD

DEPARTMENT OF ENERGY

Department of Energy
Albuquerque Operations Office
ATTN: CTID

Department of Energy
ATTN: OMA/RD&T

Department of Energy
Nevada Operations Office
ATTN: Mail & Records for Tech Lib

DEPARTMENT OF ENERGY CONTRACTORS

Lawrence Livermore National Lab
ATTN: Technical Info Dept Library
ATTN: L-504, M. Wilkins
ATTN: J. Goudreau

Los Alamos National Scientific Lab
ATTN: M/S632, T. Dowler
ATTN: MS 364

Sandia National Laboratories
Livermore National Laboratory
ATTN: Library & Security Class Div

DEPARTMENT OF ENERGY CONTRACTORS (Continued)

Sandia National Lab
ATTN: 3141
ATTN: W. Caudle
ATTN: A. Chabai
ATTN: J. Colp
ATTN: W. Herrman
ATTN: W. Altsmeirer
ATTN: W Patterson
ATTN: J. Kaizur

OTHER GOVERNMENT AGENCIES

Central Intelligence Agency
ATTN: OSWR/NED

Federal Emergency Management Agency
ATTN: Hazard Eval & Vul Red Div

NASA
AMES Research Center
ATTN: R. Jackson

U.S. Nuclear Regulatory Commission
ATTN: R. Whipp for Div of Sec for L. Shao

DEPARTMENT OF DEFENSE CONTRACTORS

Aerospace Corp
ATTN: Technical Information Services

Agbabian Associates
ATTN: M. Agbabian

Applied Theory, Inc
2 cy ATTN: J. Trulio

Avco Research & Systems Group
ATTN: D. Henderson
ATTN: P. Grady
ATTN: Library A830

BDM Corp
ATTN: Corporate Library
ATTN: T. Neighbors

Boeing Co
ATTN: Aerospace Library

California Research & Technology, Inc
ATTN: K. Kreyenhagen
ATTN: Library

California Research & Technology, Inc
ATTN: D. Orphal

EG&G Washington Analytical Services Center, Inc
ATTN: Library

Engineering Societies Library
ATTN: A. Mott

General Dynamics Corp
ATTN: R. Dibrell

General Electric Company—TEMPO
ATTN: DASIAC

Honeywell, Inc
ATTN: T. Helvig

DEPARTMENT OF DEFENSE CONTRACTORS (Continued)

Institute for Defense Analyses
ATTN: Classified Library

Kaman AviDyne
ATTN: E. Criscione
ATTN: N. Hobbs
ATTN: Library

Kaman Sciences Corp
ATTN: Library

Lockheed Missiles & Space Co, Inc
ATTN: Technical Information Center

Lockheed Missiles & Space Co, Inc
ATTN: M. Culp
ATTN: TIC-Library

Martin Marietta Corp
ATTN: H. McQuaig
ATTN: A. Cowan
ATTN: M. Anthony

Merritt CASES, Inc
ATTN: Library
ATTN: J. Merritt

Nathan M. Newmark Consult Eng Svcs
ATTN: W. Hall
ATTN: N. Newmark

University of New Mexico
Dept of Police & Parking Security
ATTN: G. Triandafalidis

Pacific-Sierra Research Corp
ATTN: H. Brode

Pacifica Technology
ATTN: G. Kent
ATTN: R. Bjork

Physics International Co
ATTN: Technical Library
ATTN: L. Behrmann

R & D Associates
ATTN: A. Field
ATTN: Technical Information Center
ATTN: P. Rausch
ATTN: W. Wright, Jr
ATTN: J. Lewis
ATTN: P. Haas

Rand Corp
ATTN: Library

Science Applications, Inc
ATTN: Technical Library

Science Applications, Inc
ATTN: W. Layson

SRI International
ATTN: J. Colton
ATTN: G. Abrahamson

DEPARTMENT OF DEFENSE CONTRACTORS (Continued)

Systems, Science & Software, Inc
ATTN: R. Sedgewick
ATTN: Library

Terra Tek, Inc
ATTN: Library

TRW Defense & Space Sys Group
ATTN: Technical Information Center
ATTN: N. Lipner

DEPARTMENT OF DEFENSE CONTRACTORS (Continued)

TRW Defense & Space Sys Group
ATTN: E. Wong
ATTN: P. Dai

Weidlinger Assoc, Consulting Engineers
ATTN: J. McCormick
ATTN: M. Baron

Weidlinger Assoc, Consulting Engineers
ATTN: J. Isenberg